Editor Decision: Reconsider after major revisions (20 Sep 2018) by Ran Feng

Comments to the Author:

Dear Authors,

Thank you for taking the initiative to improve the manuscript. I can see clear improvements to the clarity of the analysis and statistic robustness. Based on your current responses, I cannot help notice a few things waiting to be better addressed in your revised manuscript:

Response: We thank the editor for the thoughtful and constructive comments.

1. Reviewers pointed out that the simulated sea ice is low at 400 ppm CO_2 compared to published modeling studies. In your reference list, the Koenigk et al., (2013) paper suggested that for EC-Earth, September sea ice free threshold is around 500 ppm CO_2. In RCP4.5 and 2.6, EC-Earth did not reach September sea ice free by year 2100. I tend to agree with reviewers, a comparison with present-day control, and explanation of the differences are needed to validate your PlioMIP2 run.

Response: In this study we focus on understanding the warming in mid-Pliocene by comparing with the pre-industrial condition as the reference state. Following mid-Pliocene protocol, we setup our experiment as Pliocene-4-Pliocene by changing the geographical conditions, but not for Pliocene-4-future that keeping the present geographical configuration. We agree with the editor that the simulations of the warm mid-Pliocene period will provide more social relevant implications to run a Pliocene-4-future experiment, as it is regarded as an analogue to future scenario. We plan to do so in the future research using a CMIP6 model version. For current work we keep our focus on simulated mid-Pliocene climate.

We also wish to mention that the model version used for our simulations is EC-Earth 3.1, which differs from the EC-Earth CMIP5 version 2.3 as both the atmosphere model and ocean model as well as sea-ice are updated. The EC-Earth 2.3 was too cold and the cold biases are reduced in the new model. We will re-examine the sea-ice change in Arctic in new RCP4.5 and 2.6 with EC-Earth CMIP6 version.

2. Reviewers pointed out potential numeric errors in the model integration. One review noticed that this error may lead to global changes in atmospheric lapse rate. This sounds quite alarming. Please examine the lapse rate and explain whether or not this relates to different results from EC-Earth present-day and RCP runs. I wanted to point out that ERA-interim or any reanalysis data are using models to fit data, the priority of reanalysis model system is not to conserve energy. Scientific literatures were published to alarm the community not to use reanalysis blindly to perform energy balance analysis. In general, you cannot compared the energy imbalance of reanalysis data to performance of a model. A model, by design, should conserve energy.

Response: Per your suggestion, we evaluate the climatological mean and global mean of air temperature and its trend in the last 200 model years of the Pliocene run. The trend of the global mean air temperature (right panel) shows a weak positive trend in the troposphere and a weak negative trend in the stratosphere. Because of the smallness of the trend of the global mean air temperature (in the range of +/- 0.04 degree per century), plus its nearly uniform vertical structure in the troposphere (meaning little changes in the global mean lapse rate), the lapse rate feedback is thought to play little role in causing "different results from EC-Earth present-day and RCP runs".

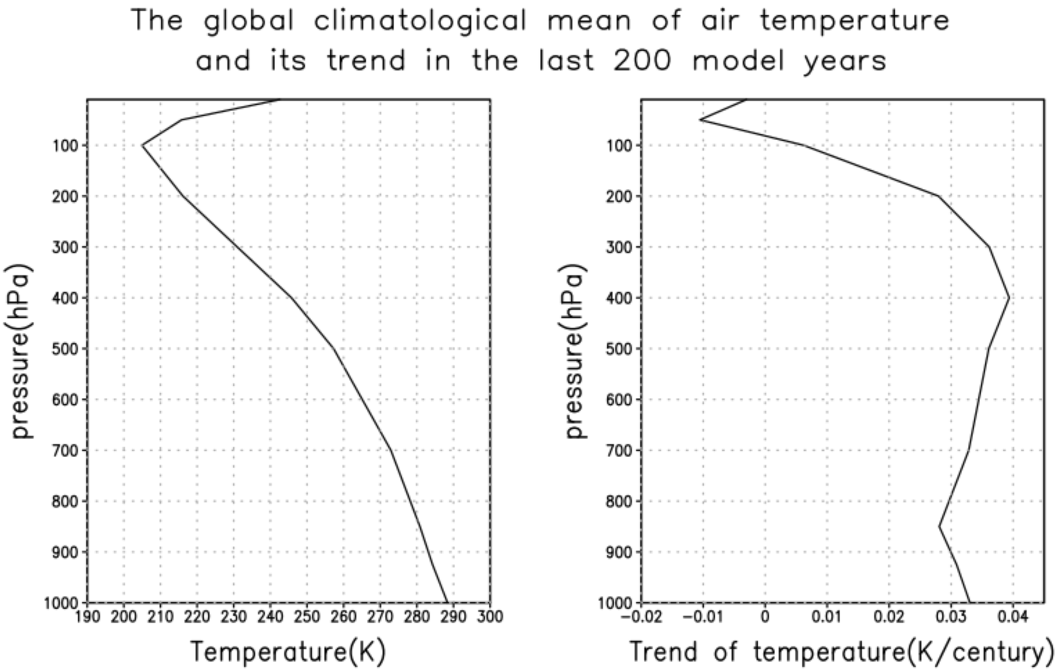

The issue of TOA and surface net radiation imbalance had been discussed in the technical report (Davini et al., 2014), which pointed out that the atmosphere loses radiation but does not cool, suggesting that the model has a "hidden" internal heating source of about 2.5 watts per square meter (in terms of global mean). It appears that the "hidden" internal heating source in the EC-Earth model is not sensitive to climate forcing, since the imbalance of the TOA radiative energy fluxes in the Pliocene run is about the same as that in the pre-industrial run. As a result, these differences in the TOA radiative energy fluxes between the two simulations actually is nearly balanced. For this reason, we think that the issue of energy imbalance at the TOA would little implication that would compromise our findings. The surface energy fluxes imbalance has been explicitly considered in our study as it is used to infer the oceanic heat uptake rate (if it is positive) or the heating release from the oceans to the atmosphere (when it is negative).

3. Reviewers pointed out that the time scale of interactions between ice and heat fluxes is below monthly. One reviewer is unsure about whether correlation at monthly scale can be used for causation arguments. Would it be possible to continue the run for another 30-yrs and run CFRAM code and spatial correlations at daily time scale? This will hopefully address

these concerns.

Response: We agree with the reviewers and Editor that “the time scale of interactions between ice and heat fluxes is below monthly” and it may be problematic to think “correlation at monthly scale can be used for causation arguments”. We here merely apply the correlation/regression analyses to estimate the strength of various feedbacks that are “coupled” with ice melting. In particular, our correlation/regression analyses reported here are performed over (horizonal) space domain, instead of temporal domain (i.e., the correlations are evaluated from plots of A versus B at different grid points in a given calendar month). From such spatial correlation/regression analyses, one could not tell “who cause who”, but infer the strength of change in A that is associated with B. Since our correlation/regression analyses are not performed over temporal domain, the temporal resolution in the data has no direct impact on the correlation/regression in terms of “degree of freedom” or “sample size”.

Of course, one may argue that the monthly mean of spatial correlations using daily data may not have the same numerical value as the spatial correlations using monthly mean data. We believe that this would be a relevant question to ask when one uses such spatial correlations for phenomena at weather scales or short-time climate scales (less than 10 years). Recall that the fields before correlation/regression analyses are the differences between two equilibrium states (one is the “pre-industrial” state and the other is the “Pliocene” state) and each of the two equilibrium states is obtained by averaging the data over 100 years. In other words, the fields that go to our correlation/regression analyses are the differences between the climatological monthly annual cycles of the two equilibrium states. Should our correlation/regression analyses be made with the difference fields between the climatological daily annual cycles of the two equilibrium states, we would construct the climatological daily annual cycles by averaging daily mean data over 100 years at a given calendar day. Because (i) the climatological daily annual cycles of both equilibrium states are already very smooth fields and (ii) the differences between the climatological daily annual cycles of the equilibrium states are regarded as the seasonal cycle of the climate response to the climate forcing imposed to the system, day-to-day variation of such seasonal cycle within each calendar month is very gradual and smooth. In this sense, we don’t expect the monthly mean of (spatial) correlations using daily annual cycle data would be different noticeably in terms of their numerical values from the (spatial) correlations using monthly mean annual cycle (which can be obtained by making monthly average of the daily annual cycle or constructing climatological monthly annual cycles from monthly mean data directly as both ways yield the same results).

Per your suggestion we have attempted to run CFRAM code at daily time scale, but it is not validated because the CFRAM is based on the energy balance of an atmosphere-surface column, and the balance is approximately maintained over the long term such as year, season and month.

4. The target time period of PlioMIP2 is mid-Piacenzian (at 3.205 Ma, belongs to the later part

of Pliocene). Pliocene epoch spans 5.3 to 2.6 Ma with varying CO_2, orbital parameters, and gateway configuration. The word "Pliocene" or even "mid-Pliocene" is inappropriate for discussing model results.

Response: The Pliocene Research Interpretation and Synoptic Mapping Project (PRISM) remains the only global-scale synoptic reconstruction of the Pliocene (Haywood et al., 2016), and PRISM data are concentrated on the warm interval (3.264-3.025 Ma). Therefore the time slice (3.264-3.025 Ma) is selected for Pliocene simulation in PlioMIP2, though the Pliocene epoch spans 5.33 to 2.58 Ma. We agree that the warm interval belongs to the late Pliocene. However, given that the mid-Pliocene Warm Period (mPWP) have been commonly used in most of the Pliocene studies, we continue using the word "mid-Pliocene" for consistency. A brief clarification has been added in Section 2.1 of the revised version.

Thank you! I am looking forward to the revised manuscript!

Davini, P., Filippi, L., and von Hardenberg, J.: Tuning EC-Earth from v3.01 to v3.1, Tech. Rep. 01/14, CNR-ISAC, UOS Torino, 2014.

Haywood, A.M., Dowsett, H.J. and Dolan, A.M.: Integrating geological archives and climate models for the mid-Pliocene warm period, Nat. Commun., 7, 1-14, doi:10.1038/ncomms10646, 2016.

Contribution of sea ~~-~~ice albedo and insulation effects to Arctic amplification in the EC-Earth Pliocene simulation

Jianqiu Zheng[1,2,3], Qiong Zhang[1], Qiang Li[1,] Qiang Zhang[1], Ming Cai[4]

[1]Department of Physical Geography and Bolin Centre for Climate Research, Stockholm University, Stockholm, 10691, Sweden
[2]School of Earth and Space Sciences, University of Science and Technology of China, Hefei, 230026, China
[3]Key Laboratory of Meteorological Disaster of Ministry of Education, Nanjing University of Information Science and Technology, Nanjing, 210044, China
[4]Department of Earth, Ocean and Atmospheric Science, Florida State University, Tallahassee, Florida, 32306, USA

Correspondence to: Jianqiu Zheng (qiu@ustc.edu.cn)

Abstract. In the present work, we simulate the Pliocene climate with the EC-Earth climate model as an ~~analogue~~equilibrium state for current warming climate induced by rising CO_2 in the atmosphere. The simulated Pliocene climate shows a strong Arctic amplification ~~featured by~~featuring pronounced warming sea surface temperature (SST) over the North Atlantic, in particular over Greenland Sea and Baffin Bays, which is comparable with geological SST reconstructions from the Pliocene Research, Interpretation and Synoptic Mapping group (PRISM~~.~~, Dowsett et al., 2016). To understand the underlying physical processes, the air~~-~~–sea heat flux variation in response to Arctic sea ~~-~~ice change is quantitatively assessed by a climate feedback and response analysis method (CFRAM) and an approach similar to equilibrium feedback assessment ~~(EFA)-like approach. Giving~~. Given the ~~facts~~fact that the maximum SST warming ~~in SST~~ occurs in summer while the maximum ~~warming in~~ surface air temperature warming happens during winter, our analyses show that a dominant ice-albedo effect is the main reason for summer SST warming, and a 1% loss in sea ~~-~~ice concentration could lead to an approximate ~~2~~1.8 Wm^{-2} increase in shortwave solar radiation into open sea surface. During winter ~~month~~months, the insulation effect induces enhanced turbulent heat flux out of the sea surface due to sea ~~-~~ice melting in previous summer months. This leads to more heat ~~release~~released from the ocean to atmosphere, thus explaining ~~the stronger~~why surface air temperature warming amplification is stronger in winter than in summer.

1 Introduction

~~Through~~As shown in the monitoring at Mauna Loa Observatory in Hawaii (https://www.esrl.noaa.gov/gmd/obop/mlo/), the CO_2 concentration in the atmosphere ~~had steadily~~ passed the 400 ppm threshold by September 2016. Accordingly, global mean temperature in 2016 increased by about 1.1 °C compared to ~~that of~~the preindustrial period, as released by the World Meteorological Organization (https://public.wmo.int/en/media/press-release~~), one~~). One major consequence of this continuing and accelerating warming is the rapid melting of ice ~~in~~at high latitudes. ~~Ten~~The ten lowest minimum Arctic sea ~~-~~ice extents since satellite records were made available in 1979 have ~~taken place in recent~~happened in every year of the last decade except for 2005, as documented by National Snow and Ice Data Centre. Moreover, an ice-free Arctic Ocean is estimated to emerge in around 2050 on the basis of climate model projections (Overland et al., 2011). As~~ the~~ sea ~~-~~ice retreats, ~~its reflectivity~~the surface of the Arctic Ocean becomes less reflective and ~~insulation decrease.~~the enhanced open-ocean region leads to greater air–sea heat exchange due to the reduced insulating effect of sea ice. This leads to ~~the ~~changes in the surface heat budget~~,~~ and~~ the~~ changes in overlying cloud and water vapour, further ~~amplify the~~amplifying Arctic warming and sea ~~-~~ice melting. Many studies have shown that the accelerated Arctic sea ~~-~~ice retreat ~~is ~~possibly ~~resulted~~results from local ice-albedo positive feedback (Winton, 2008), meridional heat transport by atmospheric circulation and oceanic current (Alexeev et al., 2013), or sea ~~-~~ice drift out of the Fram Strait (Nghiem et al., 2007; Krumpen et al., 2016). In turn, Arctic sea ~~-~~ice decline can result in a variety of impacts on climate change, such as Arctic amplification (Serreze et al., 2009), change of cloud cover and precipitation (Liu et al., 2012; Bintanja and Selten, 2014), shift in atmospheric circulation pattern (Alexander et al., 2004), and slow-down of the Atlantic Meridional Overturning Circulation (Sévellec et al., 2017). A detailed consequence of Arctic sea ~~-~~ice decline classified by local and remote effects ~~have~~has been reviewed by Vihma et al. (2014).

Such ongoing high CO_2 level and low ice concentration in the Arctic is not unique in Earth's history. Geological data show that during the Pliocene, the CO_2 concentration in the atmosphere ~~did reach~~reached 400 ppm or even more, and extreme warmth and Arctic amplification are recorded in multi-proxy evidence, including the longest and most complete record from Lake El'gygytgyn, an undisturbed Siberian lake in northeast Arctic Russia (Brigham-Grette et al., 2013). Seasonally ice-free conditions existed in some Arctic regions in the mid-Pliocene until ~~the ~~circulation through the Bering Strait reversed~~ and~~, at which point the excess freshwater supply might have facilitated sea ~~-~~ice formation (Matthiessen et al., 2009). Several climate models have simulated the Pliocene but failed to reproduce the strong Arctic amplification ~~showed~~shown in geological proxy data (Dowsett et al., 2012). While most of the previous studies on ~~contribution~~the contributions of the sea ~~-~~ice effect to Arctic amplification focus on contemporary ~~trend~~trends or future ~~projection~~projections, here the Pliocene simulation is selected ~~because of~~for three reasons: (1) The Pliocene epoch ~~(~~(approximately 3 million years ago), the most recent warm period with ~~the ~~CO_2 concentrations similar ~~CO_2 concentration as~~to today, is not only an analogue of future climate change but also an appropriate past time-slice to examine regarding sea ~~-~~ice effect (Haywood et al., 2016a). (2) The Pliocene simulation can be partly verified by proxy data reconstructed from deep-sea oxygen isotope analysis (Dowsett et al., 2012), while projecting the future ~~projection ~~from a climate model is of high uncertainty owing to the lack of any validation. (3) Whereas the historical or undergoing climate variability is transient, the Pliocene simulation is obtained after the model integration reaches ~~a ~~quasi-equilibrium~~ state~~. As inferred from Li et al. (2013), the equilibrium response is in principle reversible, while transient response is hysteretic, suggesting that the Pliocene simulation can better represent a steady climate response.

Two physical ~~attributions~~characteristics of sea ~~-~~ice are considered to affect climate system. One is much higher surface reflectivity of ice than that of open water, and the other is that ice can inhibit or reduce the exchange of momentum, heat, and mass between the atmosphere and ocean~~, hereafter~~. Hereafter we refer these two ~~attributions~~effects as "albedo" and “insulation~~ effects~~,” respectively. Most previous studies on the two effects are mainly carried out by sensitivity experiments with the atmospheric general circulation model (AGCM). For instance, Gildor et al. (2014) examined the role of sea -ice ~~on~~in the hydrological cycle using the Community Atmospheric General Circulation Model (CAM3). ~~Two~~The two effects are separated by modifying the sea -ice albedo to that of open-water, or setting the sea -ice thickness to zero ~~but its albedo~~ and keeping albedo unchanged. Their results show that the insulation effect on the hydrological cycle is larger than the albedo effect, and these two effects are not independent, i.e. their total effect is not the sum of their separate contribution. Lang et al. (2017) also pointed out that the sea -ice thinning in recent years can lead to a 37% increase~~ 37%~~ of Arctic amplification through the enhanced insulation effect, as estimated by an AGCM. Note that sea surface temperature (SST) is prescribed in their AGCM simulation, while sea -ice albedo or thickness is modified. In fact, the modification of sea -ice does not closely match the fixed SST~~ closely~~, which may lead to a bias in the sea -ice effect estimation from the AGCM simulation. The climate system, in turn, reinforces sea -ice loss while influenced by albedo or insulation ~~effect~~effects, which ~~is~~are known as ice~~-~~–albedo feedback or ice~~-~~–insulation feedback. In addition, albedo ~~effect~~ and insulation ~~effect interacts~~interact in a nonlinear way (Gildor et al., 2014). These feedbacks and ~~interaction~~interactions add more challenges to ~~understand~~understanding the effect of sea -ice on climate. Recently, Burt et al. (2016) and Kim et al. (2016) addressed the relationship between sea -ice loss and air~~-~~–sea interface heat budget using the Community Earth System Model (CESM) simulation and cyclo-stationary empirical orthogonal function (CSEOF) analysis, respectively. However, the studies contain large uncertainties due to the hysteresis of transient processes (Li et al., 2013). Although the surface heat budget is the most fundamental ~~to~~ aspect of air~~-~~–sea interaction, it is still not clear to what ~~degree~~extent heat flux responds to the change of Arctic sea -ice. Therefore the present study aims to quantitatively assess the variation of each individual component of air~~-~~–sea heat flux caused by the decrease of Arctic sea -ice albedo and insulation. The analysis is based on the EC-Earth simulation of the Pliocene climate, which ~~representing~~represents an analogue for a future climate at equilibrium ~~climate~~with modern greenhouse gas levels, and the reference state is preindustrial equilibrium climate state.

The remainder of the paper is organized as follows. Section 2 describes the EC-Earth model and experimental design, and introduces the climate feedback and response analysis method (CFRAM~~),~~) as well as the approach to extract the impact ~~contributed from~~of sea -ice loss. In ~~section~~Section 3, we present several climate features simulated in the Pliocene experiment. The albedo and insulation effects of sea -ice on air~~-~~–sea interface heat flux are investigated in Sections 4 and 5, respectively~~ in sections 4 and 5, ~~, followed by summary and discussion in ~~section~~Section 6.

2 Model and method

2.1 Model description and experimental design

The model applied in the study is the global coupled climate model EC-Earth (version 3.1, Hazeleger et al., 2012). Its atmospheric component is the Integrated Forecast System (IFS, version cycle 36r4) developed at the European Centre for Medium-Range Weather Forecast (ECMWF), including the land model H-TESSEL (Balsamo et al., 2009). This atmospheric spectral model is run at T159 resolution (roughly 1.125°, ~~∼~~approximately 125 km) with 62 vertical levels and coupled to ~~the~~an ocean component~~ that is~~ based on the Nucleus for European Modelling of the Ocean (NEMO, version 3.3, Madec, 2008) and the Louvain-la-Neuve sea ~~-~~ice Model (LIM, version 3, Vancoppenolle et al. 2009). ~~The~~ NEMO ~~is~~was developed at the Institute Pierre Simon Laplace (IPSL) and has a resolution of about 1° and 46 vertical levels. In LIM3, surface albedo parameterization follows Shine and Henderson-Sellers (1985~~),~~) with the following values: thick dry snow 0.8, thick melting snow 0.65, thick frozen bare ice 0.72, thick melting bare ice 0.53, and thin melting ice 0.47. The tuning of bare ice and snow albedo would affect whether the equilibrium ice thickness is reasonable and whether the ice is from a multi-year or seasonal ice zone. The coupling between the atmosphere and ocean/sea ~~-~~ice is through the Ocean Atmosphere Sea ~~-~~ice Soil coupler (OASIS, version 3.0, Valcke, 2006). EC-Earth has been used to examine the Arctic climate for the historical period and future scenarios in CMIP5. An evaluation of EC-Earth for the Arctic shows that the model simulates the 20th century Arctic climate reasonably well. EC-Earth simulated cloud variables with slightly larger cloud fraction and less cloud condensate ~~compared to~~than ERA-Interim, which ~~lead~~led to similar longwave cloud radiative forcing. Moreover, total cloud forcing in EC-Earth is in good agreement ~~to~~with the APP-x satellite estimates (Koenigk et al., 2013). Koenigk et al. (2013) showed that the annual mean surface temperature in the Arctic increases by 12 K in the EC-Earth RCP8.5 scenario simulation, and the most pronounced warming is during autumn and winter in the lower atmosphere. A likely ice-free Arctic is indicated in September around 2040. The enhanced oceanic meridional heat flux into the Arctic (Koenigk et al., 2013) and the enhanced atmospheric northward latent energy transport (Graversen and Burtu, 2016) are suggested as major contributors to ~~the~~ future Arctic warming in the EC-Earth simulation. ~~Recently the~~The EC-Earth model ~~is~~has also been applied to understand ~~the~~ past ~~climate~~climates, such as changes in the~~ change of~~ Arctic climate (Muschitiello et al., 2015), African ~~monsoon~~monsoons (Pausata et al., 2016; Gaetani et al., 2017), tropical ~~cyclone~~cyclones (Pausata et al., 2017a~~)~~), and ENSO activity (Pausata et al., 2017b) during the mid-Holocene. In this study we apply the model to the mid-Pliocene climate and focus on the effects of sea ~~-~~ice on Arctic climate change.

Two numerical experiments are performed with EC-Earth to facilitate this study. One is the preindustrial control run with the 1850 CO_2 concentration of 284.725 ppm, and the other is the mid-Pliocene warm period (3.264–3.025 Ma) sensitivity experiment in which the atmospheric CO_2 concentration is set to 400 ppm. The PRISM remains the only global-scale synoptic reconstruction of the Pliocene (Haywood et al., 2016a), and PRISM data are concentrated on the warm interval (3.264–3.025 Ma). Therefore the time slice (3.264–3.025 Ma) is selected for Pliocene simulation. Though the warm interval belongs to the late Pliocene, given that the mid-Pliocene warm period have been commonly used in most of the Pliocene studies, here we continue using mid-Pliocene for consistency. Following the protocol of the Pliocene Model Intercomparison Project, phase 2 (PlioMIP2, Haywood et al., 2016b), several configurations are modified in the Pliocene simulation: (1) in the Pliocene experiment, all ~~other~~ trace gases ~~except~~other than CO_2, such as CH_4~~ and~~, N_2O, and aerosols~~ in the Pliocene experiment~~, are specified ~~to be~~as identical to the preindustrial run~~.~~ to account for the absence of proxy data. (2) Orbit forcing, including eccentricity, obliquity, and precession, remains same ~~with~~in the preindustrial run~~.~~ as in the mid-Pliocene warm period, which has a near-modern orbital forcing. (3) Enhanced boundary ~~condition~~conditions from the Pliocene Research, Interpretation and Synoptic Mapping group (PRISM, Dowsett et al., 2016~~)~~), including land–sea mask, topography, bathymetry, and ice-sheet, are applied in the Pliocene experiment~~ where the land-sea mask, orography, bathymetry, vegetation~~. The global distributions of lake, soil, and ~~ice-sheet~~biome are modified ~~accordingly.~~to match the new land–sea mask and ice reconstruction. The integrations of the preindustrial control run and the Pliocene experiment are carried out for 500 years, and it takes ~~approximate~~approximately 300 years for the model to reach equilibrium. From our last 200 years of output in the Pliocene simulation (see Figure S1 in the Supplement), the mean top of the atmosphere (TOA) net radiation is about ~~-~~–0.5 Wm^{-2} and its trend is near zero. The trend of mean SST is about 0.027 K/century, which fulfils the PMIP4 criterion that the trend of mean SST should be less than 0.05 K/century (Kageyama et al., 2018). In this study, the last 100-year-mean of all variables are used for analysis, and the Pliocene climate anomalies are calculated ~~with respect to~~by subtracting the mean of the preindustrial ~~control run. The Arctic in~~simulation without trends removal. In the following analysis, the Arctic is defined as the region poleward of 70 °N.

2.2 Climate feedback and response analysis method (CFRAM)

~~Radiative forcing varies as CO_2 concentration increases~~Climate system warming in the Pliocene experiment is driven by variation in radiative forcing, which ~~drives climate system warming.~~is in turn caused by increased CO_2 concentration. In response to temperature change, factors such as surface albedo, cloud, water vapour, and air temperature will adjust and feedback until the climate system reaches equilibrium. The contribution from each factor can be quantitatively evaluated by climate feedback analysis. ~~The traditional~~Traditional climate feedback analysis ~~method~~methods, such as partial radiative perturbation~~ (PRP) technique~~, is based on TOA radiative budget (Wetherald and Manabe, 1988), while the radiative kernel method can be extended to the surface and remain computationally efficient (Soden and Held, 2006; Pithan and Mauritsen, 2014). However, none of them takes individual physical processes into account, particularly non-radiative processes. ~~The climate feedback and response analysis method (~~CFRAM~~)~~, proposed by Lu and Cai (2009~~)~~), overcomes this limitation.

CFRAM contains two parts: one is decomposing radiative perturbation into individual contribution, including shortwave and longwave components, from CO_2, surface albedo, cloud, water vapour, and air temperature~~. It~~:

$$\Delta Q_{rad} = \Delta(S+R)_{co_2} + \Delta S_{albedo} + \Delta(S+R)_{cloud} + \Delta(S+R)_{WV} + \Delta R_T \quad , \quad (1)$$

where ΔQ_{rad} is ~~performed by offline calculation using~~total radiative ~~transfer model (Fu and Liou, 1993) with~~flux perturbation at the ~~output from~~surface (ice and ocean), ΔS and ΔR are the ~~preindustrial control run and~~ net shortwave and longwave radiative perturbations at the ~~Pliocene sensitivity experiment.~~surface, respectively, and the subscripts CO_2, albedo, cloud, WV, and T represent the partial radiative perturbation due to changes in the CO_2 concentration, surface albedo, cloud properties, atmospheric water vapour, and air temperature, respectively. Note that here it is assumed that the interactions among the factors (CO_2, surface albedo, cloud, water vapour, and air temperature) are negligible and the higher order terms of each factors are omitted. The other part is calculating partial ~~temperate~~temperature perturbation due to individual radiative and non-radiative feedback processes, which is based on total energy balance and derived from the relationship between longwave radiation and temperature change. A more detailed description about CFRAM can be found in Lu and Cai (2009).

CFRAM is a practical diagnostic tool to ~~analyze~~analyse the role of various forcing and feedback agents and has been used widely in climate change research (e.g. Taylor et al., 2013; Song and Zhang, 2014; Hu et al., 2017). In the present study, total radiative flux perturbation is first calculated from the surface radiative flux difference between the Pliocene sensitivity experiment and the preindustrial control run. Then we apply the first part of CFRAM to ~~obtain the surface radiative flux~~ compute each partial radiative perturbation, which is performed by offline calculation using a radiative transfer model (Fu and Liou, 1993). The linear approximation in Equation (1) should be verified with the output from the radiative transfer model. Finally, the partial radiative perturbation due to albedo, cloud, and water vapour~~, and link it~~ can be used to evaluate albedo or insulation ~~effect~~effects of sea-ice.

2.3 Approach to extract sea-ice effects

As sea-ice declines in the Pliocene warming climate, air–sea heat flux ~~at air-sea interface~~ varies. However, the variation is not only due to the impact of sea-ice but also determined by other factors, such as atmospheric circulation. Therefore an approach capable of quantifying the influence of a factor is indispensable ~~to extract~~for extracting the corresponding ~~part~~contribution of sea-ice effect from the total heat flux change. To distinguish sea-ice's contribution from the other processes, the linkage between sea-ice and heat flux needs to be identified through either temporal correlation or spatial correlation, if the effect of sea-ice is assumed to be linear. A canonical case of the former is ~~the~~ equilibrium feedback assessment (EFA~~) method,~~), which has been used to quantify the influence of sea-ice on cloud cover (Liu et al., 2012) and the heat flux response to SST (Frankignoul and Kestenare, 2002).

Here we adopt a method similar to EFA, but built on spatial correlation due to the limitation of data and computation. As a high-temporal–resolution CFRAM calculation, such as 6-hourly or daily, is computationally expensive, monthly data are used in the analysis. However, the monthly resolution is too coarse to explain the relationship between heat fluxes and sea-ice concentration by temporal correlations. Therefore, spatial correlations are calculated. This method is used in Hu et al. (2017) to correct cloud feedback. The response of heat flux to ~~change~~changes in sea-ice concentration (SIC) is represented as

$$F(s)=\lambda I(s)+N(s), \qquad (\cancel{1)}2))$$

where $F(s)$ is the heat flux anomaly at location s, $I(s)$ is anomalous SIC, λ is the response coefficient of heat flux to SIC change, and $N(s)$ is the climate noise independent of SIC variability. The response coefficient can be calculated as

$$\lambda=\frac{cov[F(s),I(s)]}{cov[I(s),I(s)]}, \qquad (\cancel{2)}3))$$

where $cov[F(s), I(s)]$ is the spatial covariance between heat flux and SIC, and $cov[I(s), I(s)]$ is the spatial variance of SIC.

The statistical significance of response coefficient is tested using a two-sided Student's t-test, where the effective degree of freedom is estimated from the auto-correlation function (Bretherton et al., 1999) as

$$n = N\frac{1 - r_1 r_2}{1 + r_1 r_2}, \quad (\cancel{3}4)$$

where n is the effective degree of freedom, N is the sample size, and r_1 is the lag-one auto-correlation of heat flux ~~and~~ (similarly r_2 for SIC~~.~~). Note that auto-correlation of heat flux and SIC is so strong that r_1 and r_2 can approach 1, leading to a ~~drastically~~drastic decrease of effective degree of freedom.

3 Mid-Pliocene climate features

Unlike the ~~present earth~~modern Earth observation system, the Pliocene climate proxy data are reconstructed mainly from the ~~benthic~~ oxygen isotope analysis of deep-sea samples, such as forminifera, diatom, and ostracod assemblages. Several climate features have been revealed with the multi-proxy data~~, one~~ (Haywood et al., 2016a). One of the most ~~concern is permanent El Niño-like condition during the mid-Pliocene warm period (Wara et al., 2005; Federov et al, 2006), which points out that the SST difference between the western and eastern equatorial Pacific was absent or less evident, similar to the contemporary El Niño SST pattern while not happening on interannual timescale. The other characteristic~~concerning is Arctic amplification — the warming in surface air temperature (SAT) in the Arctic region tends to be more than twice as warm as that in the low- and mid-latitude ~~region~~regions (Serreze and Barry, 2011). ~~However, the~~Furthermore, Arctic SAT and SST during Pliocene is significantly warmer than today~~ even though they have~~, despite comparable CO_2 ~~concentration~~concentrations (Ballantyne et al., 2013~~), which~~). This probably stems from the fact that the present transient process ~~that~~ has not yet reached a steady state, or is due to the change of~~ the~~ gateways that can affect the Atlantic meridional overturning circulation (AMOC) (Brierley and Fedorov, 2016; Otto-Bliesner et al., 2017; Feng et al., 2017).

In Figure 1, we show the ~~changes in~~annual mean warming and seasonal warming averaged over the Arctic Ocean for SST and SAT between the Pliocene and preindustrial ~~period and the Pliocene epoch.~~simulations. The shaded circles in the SST change distribution (Figure 1a) represent the mean annual SST anomalies at 95% confidence-assessed marine sites from the Deep Sea Drilling Project ~~(DSDP)~~ and Ocean Drilling Program~~ (ODP),~~, which are available in the supplementary table of Dowsett et al. (2012). The overlay of proxy data over the filled contour maps does not show the difference well, so the difference of annual mean SST anomaly between EC-Earth simulation and the proxy data is shown in Figure S2. In contrast to the large underestimation of multi-model ensembles ~~to~~regarding the warming over the northern Atlantic sector of the Arctic Ocean (Dowsett et al., 2012), the warming amplitude and pattern in EC-Earth simulation is comparable with the high-confidence proxy data. This is consistent with the ~~results~~result of Koenigk et al. (2013), which ~~pointed out~~suggests that the sea ice change in EC-Earth is strong and that the EC-Earth simulations show a strong Arctic amplification compared to most CMIP3 models. ~~Meanwhile, a warming can be seen along the coastal upwelling zones off the America, which implies a permanent El Niño-like feature.~~ According to Figure 1b, the Pliocene SAT north of 70 °N is as much as 10~~-~~–18 °C higher than the preindustrial period, similar to the mid-Pliocene paleoclimate estimate by Robinson et al. (2008).

~~Figure~~Figures 1a and 1b also show that the SST and SAT anomaly patterns are somewhat similar over low- and mid-latitude ~~region, but they are apparently~~regions, different from over high-latitude ~~region~~regions, particularly over the Arctic Ocean, which ~~is~~was previously illustrated by Hill et al. (2014). This disparity results from the intense air~~-~~–sea coupling over tropical and subtropical ~~ocean~~oceans, while the air~~-~~–sea interaction is relatively weak over the Arctic Ocean owing to the albedo and insulation effects of sea ~~-~~ice. ~~Noteworthily, the~~Notably, SST warming~~ of SST~~ averaged over the Arctic Ocean shows a distinct seasonal evolution from that of SAT~~, and~~; the maximum warming in SST occurs in summer, while the maximum warming in SAT happens during winter (~~Figure~~Figures 1c and 1d).

~~The SIC is very sensitive during the different period as shown in Figure 2a-c.~~ During the preindustrial period, the annual mean sea ~~-~~ice appears to cover the whole Arctic Ocean except for the Greenland Sea, the Norwegian Sea, and the Barents Sea, and it retreats to the western Arctic Ocean in the Pliocene, leading to a significant decrease of sea ~~-~~ice extent over the Fram Basin and Baffin Bay~~.~~ (Figures 2a–c). Consequently, the net ~~air-sea interface~~ heat exchange at the surface of ice or ocean varies greatly (Figure 2d~~-f). The sea-ice~~–f). The net heat flux and other flux terms mentioned hereafter are defined as positive downward. A positive value means that the ocean gains heat from the atmosphere and a negative value means oceanic heat loss. The net heat flux over the sea ice–covered area ~~seems to be~~clearly shows net heat loss during both the preindustrial period and the Pliocene~~.~~ (Figures 2d and 2e). Thus, it can be expected that net heat gain will occur when the sea ~~-~~ice declines. However, the Fram Basin and Baffin Bay ~~displays~~display pronounced heat loss, which might be linked to the disappearance of sea ~~-~~ice in the Pliocene (Figure 2b).

The net heat flux at the ~~air-sea interface~~surface of ice or ocean can be ~~written~~represented as

❑□ ❑□ ❑□ ❑□ ❑□~~, (4)~~

~~Where~~ Q_{sw} ~~and~~ Q_{lw} ~~are~~ the sum of four terms: the net ~~solar~~ shortwave ~~and~~ radiative flux, the net longwave radiative ~~heat fluxes,~~ Q_{sh} ~~and~~ Q_{lh} ~~are~~flux, the turbulent sensible heat flux, and the turbulent latent heat ~~fluxes. All terms are defined positive downward. Therefore, the positive value means that ocean gains heat from the atmosphere and the negative value means oceanic heat loss.~~

~~—~~flux. Figure 3 compares the annual mean of the four ~~components of surface heat~~ flux terms to further illustrate the possible relationship between sea ~~-~~ice and net heat exchange (~~Figure~~Figures 2c and 2f). The radiative and turbulent heat ~~fluxes~~flux anomalies both are positive over the Chukchi Sea, ~~thereby~~indicating a marked net heat gain emerging there. Over the Beaufort Sea and East Siberian Sea, the positive change in the net shortwave radiation ~~is~~anomalies are dominant over the other three negative components, yielding ~~the~~ net heat gain. ~~On the contrary~~In contrast, the positive net shortwave radiation anomalies over the Fram Basin, the Greenland Sea, and Baffin Bay ~~is~~ are less than the sum of net longwave radiation and turbulent heat ~~fluxes~~flux anomalies, thus leading to net heat loss. The negative turbulent heat ~~fluxes~~flux anomalies over Fram Basin, the Greenland Sea, and Baffin Bay are ~~so~~ prominent, indicating the sea ice effect on turbulent heat ~~fluxes~~flux anomalies in light of the transition to ice-covered or ice-free ~~state~~ states, respectively. ~~As shown in~~Note that the partition threshold of ice-free and ice-covered conditions is 15% SIC, i.e., a grid point with an SIC of less than 15% is considered ice-free. In Figure 2c, the diagonal stripe represents the region with the transition from ice-covered to ice-free condition, and the diagonal crosshatch represents the region ~~remaining~~that retains its ice-covered status as the simulation shifts from the preindustrial period to the Pliocene. Only ice-covered regions are examined, as there appears to be large surface heat flux changes in regions that contain no sea ice in both periods, which could be contaminating the statistical relationships between sea ice and the associated surface flux changes.

4 Albedo effect of sea ice

Arctic amplification has been demonstrated by significant SAT anomalies in the foregoing Pliocene simulation~~, and it can be accounted as the synergy of CO_2 external forcing and feedback effects associated with~~. Similar to the process-based decomposition of a climate difference in Hu et al. (2017), the SAT anomalies in the Pliocene simulation as compared to the preindustrial simulation can be thought of as the combination of partial temperature perturbations due to radiative feedbacks (surface albedo, cloud, water vapour, and air temperature~~.~~) and non-radiative feedbacks (surface sensible and latent heat fluxes, dynamical advection, ocean processes, etc.). That is to say, the albedo effect of sea ice and snow can be quantified by climate feedback analysis such as CFRAM. ~~The surface~~ Surface albedo is defined as the ~~ratio~~proportion of the ~~reflected to the incoming~~incident solar shortwave radiation that is reflected by the surface, therefore indicating that albedo effect is relevant ~~with~~to net shortwave radiation rather than net longwave radiation and turbulent heat fluxes.

The annual mean net shortwave radiation change due to sea ice and snow albedo derived from CFRAM is presented in Figure 4. The largest net shortwave radiation change exceeding 50 Wm^{-2} takes place over ~~the~~ Fram Basin and Baffin Bay, and most of the Arctic Ocean, except for part of the North Atlantic and the Barents Sea ~~show~~, shows net shortwave radiative heat gain. ~~Comparing~~Compared with the SIC change (Figure 2c), the increase of annual mean net shortwave radiation absorbed by the ocean is in accordance with sea ice retreat, which can be clearly depicted in a scatter plot (Figure 5). ~~The high~~The effective degree of freedom is calculated from Formula (4) for testing statistical significance, and the correlation coefficient (r~~=-~~ = −0.~~92)~~84) is significant at a 99% confidence level. This indicates that changes in sea ice extent can explain the approximate ~~84~~71% (square of correlation coefficient) variance of total shortwave radiation change due to albedo, and the residual variance may be caused by changes in snow cover ~~or~~and sea ice/snow state as well as thickness. The statistically significant response coefficient calculated according to formula (~~2~~3) is ~~-46.5~~ −43.0 Wm^{-2} ~~(exceeding 99% confidence level),~~, indicating that a 1% decrease in annual mean SIC leads to an approximate 0.~~5~~43 Wm^{-2} increase in net shortwave radiative heat flux at the surface.

~~Regarding the seasonal variation of~~As SIC and~~ the~~ incoming solar radiation ~~are distinct~~ in the polar region vary with season, we examine the response of net shortwave radiation to sea ~~-~~ice change for every month. As shown in Figure 6, the response coefficient of albedo to SIC displays a seasonal variation, peaking in ~~which it peaks in May~~June with ~~the~~a maximum absolute value ~~188.1~~of 178.3 Wm^{-2} (approximate ~~2~~1.8 Wm^{-2} increase in net shortwave radiation due to 1% decrease in SIC). The prominent oceanic heating in May and June seems ~~inconsistent~~consistent with the maximum SST warming in August, as the response of seawater lags about 2 months behind due to the great heat inertia and heat capacity of seawater (Venegas et al., 1997; Zheng et al., 2014). Even though Arctic sea ~~-~~ice itself has a great variability owing to melting and freezing processes, ~~the~~ SIC anomalies do not exhibit a large variability in different seasons, ranging from 0.~~34~~19 to 0.~~44~~26 as shown in the standard deviation of SIC (Table 1). However, the standard deviation of net shortwave radiation anomalies (with respect to monthly mean) associated with albedo effect varies from ~~88.43~~52.45 Wm^{-2} in May to 0 Wm^{-2} in December, when the polar night ~~occurring~~occurs without any sunlight. Moreover, ~~it is found from~~our correlation analysis indicates that sea ~~-~~ice has a statistically significant impact on surface shortwave radiation, except in November, December, and January, when there is low incident solar shortwave radiation during the Arctic winter. Overall, the seasonality of sea ice's albedo effect ~~of sea-ice~~ on surface shortwave radiation is attributed primarily to the seasonal cycle of net shortwave radiation, and the contribution of ~~sea-ice~~SIC variation is substantially small.

5 Insulation effect of sea ~~-~~ice

5.1 Insulation effect of sea ~~-~~ice on surface radiation

The ~~insulation~~insulating effect of sea ~~-~~ice~~,~~ has an indirect effect on the net surface shortwave and longwave fluxes. By separating the overlying atmosphere from the ocean, ~~does not affect surface shortwave or longwave radiation directly. In fact, the insulation~~sea ice reduces ~~the~~ evaporation from the ocean~~ to atmosphere~~, resulting in a decrease ~~of~~ in water vapour and cloud cover~~, and thus playing~~. This reduction plays a non-negligible role ~~on~~ in the amount of downward shortwave and longwave radiation reaching the surface~~ radiation~~. However, ~~the water vapour and cloud contain a mixture of local evaporation and~~ remote moisture transport~~. In~~ also affects water vapour and cloud amount. Thus, in order to address the insulation effect of sea ~~-~~ice, two steps have to be performed. First, we obtain the total influence of water and cloud on surface radiation by CFRAM. Second, we need to extract the contribution from a local source associated with sea ~~-~~ice.

Figure 7 shows the annual mean cloud feedback and water vapour feedback on net shortwave and longwave radiation, respectively~~.~~, before removing the remote effects on clouds and water vapour. Even though ~~the~~an increase in cloud cover is expected with the diminishing Arctic sea ~~-~~ice (Liu et al., 2012), whether the increased cloud cover will heat or cool the surface depends on the cloud characteristics~~ of cloud~~. The cloud feedback on shortwave radiation is nearly out of phase with that on longwave radiation, except in the Beaufort Sea and the East Siberian Sea (Figure 7a, 7b). The significant decrease of low cloud cover in the North Atlantic (Figure S3a) may enhance incoming shortwave radiation and weaken downwelling longwave radiation, thus contributing to the positive anomaly in shortwave radiation and negative anomaly in longwave radiation in the North Atlantic. Similarly, the increase of high cloud cover east and north of Greenland (Figure S3b) is responsible for the positive anomaly in longwave radiation over the related areas. In contrast, ~~the~~ water vapour feedback tends to simultaneously cool and heat the surface by absorbing solar radiation and ~~heat the surface by~~ downwelling longwave radiation, ~~and~~respectively; the ~~latter~~ heating is one order of magnitude higher than the ~~former~~ cooling (Figure 7c, 7d).

The approach to extract the ~~counterpart of sea-ice~~ local insulation effect due to changes in sea ice concentration is based on the premise that the insulation effect on surface radiation is linear with SIC. Like the steps performed ~~in~~to isolate the albedo effect, the response coefficient of shortwave and longwave radiation due to cloud and water vapour for annual mean and seasonal evolution can be calculated respectively, and the results are shown in Figure 8. ~~As to~~In the annual mean, the main contributor comes from cloud feedback on longwave radiation ~~(-12.6~~(–11.1 Wm^{-2}), and the cloud feedback on shortwave radiation and water vapour feedback on longwave radiation are similar in magnitude, but opposite in sign. In addition, the annual mean absorption of incoming solar radiation by water vapour is negligible, and this is true for the individual month as well. The absorption and reflection of shortwave radiation by cloud ~~represents~~shows a pronounced seasonal cycle, with a large effect in ~~July and~~ August. However, there is no statistically significant relationship between ~~SIC and~~ cloud feedback on shortwave radiation and SIC (Table 2). ~~Comparing~~Compared to the seasonal variation of ~~shortwave radiation change,~~ standard deviation of the net shortwave radiation anomalies, standard deviation of the net longwave radiation anomalies caused by cloud and water vapour associated with local SIC anomalies both show smaller seasonal variation, therefore leading to a relatively constant contribution of sea -ice insulation to surface longwave radiation, except in summer months when there is a lack of ~~significant interaction~~linear relationship between SIC and longwave radiation (Table 2). Note that the longwave cloud forcing in September (–17.6 Wm^{-2}) is quite large relative to all the other months, which might result from the maximum cloud cover over the Arctic, as well as the fact that the linear relationship between sea ice concentration and longwave radiation changes due to cloud is strongest in September.

5.2 Insulation effect of sea -ice on turbulent heat fluxes

~~The air-~~Air–sea turbulent heat fluxes, including sensible and latent heat fluxes, have been widely studied with the bulk aerodynamic formula, which specifies that the turbulent heat fluxes are dependent on surface wind speed, sea surface and air temperature difference, specific humidity difference, and the bulk heat transfer coefficient. However, due to the existence of sea -ice, the Arctic turbulent heat fluxes show distinctive features from ice-free ~~condition~~conditions, which has been mentioned in Section 3. It is therefore essential to take the insulation effect of sea -ice into account and differentiate ~~ice-covered flux~~fluxes from ice-covered versus ice-free ~~one.~~areas. This is demonstrated in Figure 9, which displays the Pliocene anomalies in annual mean sensible and latent heat ~~flux change~~fluxes as a function of SIC anomalies. There ~~are~~ is a larger ~~spreads of~~ spread in the turbulent heat flux ~~change~~anomalies over the ice-free ~~area~~areas (grey symbols, corresponding to the diagonal hatched region in Figure 2c) than ~~that of~~ in anomalies from the ice-covered~~,~~ areas (light blue symbols, cross-hatched region in Figure 2c) because the former is free from the constraint of sea -ice. The constraint of sea -ice can be apparently captured through the scatter plot of turbulent heat flux and changes in SIC ~~change (the~~ (light blue ~~plot in Figure 9,~~

~~corresponding to the diagonal crosshatch~~symbols). For the ice-covered areas~~ in Figure 2c), and~~, SIC can explain approximate 59% and 74% (square of correlation coefficient) of the variance in the sensible heat flux and latent heat flux, respectively.

The linear regressions of sensible and latent heat flux anomalies on SIC are similar but different. The response coefficient of sensible heat flux (35.3 Wm^{-2}) to SIC is larger than that of latent heat flux (27.7 Wm^{-2}~~)~~) for the ice-covered areas, which means that the sensible heat flux is more sensitive to SIC change than the latent heat flux. ~~Noteworthily~~Notably, this is different from the turbulent heat flux variability over low- and mid-latitude regions, where the ~~trend~~variability of sensible heat flux is significantly less than that of latent heat flux~~ (e.g., ~~, such as the trend of turbulent heat flux over the low- and mid-latitude North Pacific and North Atlantic oceans from 1984–2004 (Li et al., 2011). The positive intercept on the turbulent flux anomaly axis implies more heat gain at the sea surface, even ~~if there is no~~without SIC change. Because the large specific heat capacity of seawater leads to less warming of the ocean than of the atmosphere, ~~therefore~~ the sea surface and air temperature difference ~~or~~ (the specific humidity difference) decreases ~~in~~during the cold season when the turbulent heat transport is the most pronounced, ~~and~~ consequently resulting in ~~the less~~a lower annual heat loss from the ocean to the atmosphere.

Figure 10 shows the seasonal response coefficient of the sensible and latent heat fluxes to the ~~sea-ice. Apparently two~~ SIC. It appears that the turbulent heat fluxes have ~~the~~a similar seasonal evolution, peaking in November and showing a negative response in July. Therefore~~ the maximum warming of SAT occurs in November as a consequence of ~~, the prompt atmospheric ~~prompt~~ response to turbulent heating~~.~~ is an important contributing factor to the maximum SAT warming that occurs in November. The melting of sea~~-ice~~ ice due to warming by high levels of CO_2 can attenuate the insulation effect and result in more heat transfer through the processes of conduction or evaporation from the ocean to the atmosphere when SST is higher than SAT~~,~~; therefore, the turbulent heat fluxes correlate positively with SIC in all seasons except summer (Table 3). If SAT is higher than SST~~,~~ (for instance, in July~~ the~~), sea ~~-~~ice will inhibit the heat transfer from the atmosphere to ocean~~,~~; thus, the negative correlation emerges. However, the correlations between the turbulent heat fluxes and SIC in summer are not statistically significant (Table 3), indicating other factors ~~might be dominant~~ rather than sea ~~-~~ice might be dominant.

6 Summary and discussion

~~In the present work we attempt to understand the albedo and insulation effects of sea-ice, on a warm Arctic climate during Pliocene simulated by EC-Earth coupled model. In contrast to~~Arctic amplification in the Pliocene has previously been addressed from reconstructed data (e.g. Robinson et al., 2008; Brigham-Grette et al., 2013); however these data tell only part of the story because of a scarcity of data sites. A model may be applied to investigate mechanisms and processes that help understanding. In contrast to the underestimation of multi-model ensembles documented in Dowsett et al. (2012), the EC-Earth Pliocene simulation can better display some ~~main features manifested in the~~ characteristics that have been revealed by the paleoclimate proxy data from deep-sea oxygen isotope analysis. Thus the EC-Earth coupled model is used in the present work to simulate the Pliocene climate and study the contribution of sea ice albedo and insulation to Arctic amplification~~ in Pliocene had been confirmed by reconstructed data (e.g. Robinson et al., 2008; Brigham-Grette et al., 2013). Proxy data,~~

~~however, tell only part of the story. Thus a model is applied and it can reveal the complete picture with reasonable explanation~~.

~~As a key to reveal the important features of Arctic amplification, the air-~~Air–sea heat flux variation in response to Arctic sea -ice change is quantitatively assessed by CFRAM and an EFA-like method~~.~~ in order to reveal important features of Arctic amplification. Table 4 summarizes the results presented in ~~section~~Sections 4 and 5, which separately ~~illustrated~~illustrate the effects of changes in albedo and insulation of sea -ice on surface heat exchange. Annual mean and seasonal evolution of effects are both considered~~, and~~. These allow us to partly interpret the mechanisms of Arctic amplification because the results are merely the contribution from sea -ice change. A complete energy budget, including dynamical and thermodynamical processes, is required to understand Arctic amplification comprehensively.

The Pliocene Arctic amplification compared to the preindustrial simulation represents a maximum SST warming in August and ~~expected to partly interpret the variability of heat flux.~~

~~The albedo~~a maximum SAT warming in November, which might be associated with the albedo and insulation effects of sea ice. Albedo only regulates the shortwave radiation, and its effect is primarily determined by annual cycle of insolation. As sea -ice melts ~~from~~starting in early spring, the enhanced insolation through open sea surface makes the ocean warmer, with the most pronounced heating anomalies in May and June. Because of the great heat inertia and heat capacity of seawater, the SST ~~warming~~anomaly peaks in August. As a result of the albedo effect of sea -ice, ocean heat content increases and more heat is stored in the upper ocean, which is the potential for the later enhanced heat release from ocean to atmosphere. The insulation effect of sea -ice can indirectly modulate ~~not only~~ shortwave and longwave radiation anomalies indirectly through cloud and water vapour~~, but also~~ as well as directly modulate sensible and latent heat ~~fluxes directly~~ flux anomalies, since sea -ice serves as a barrier. Averaged over the year, the absorption of longwave radiation due to insulation effect is about 4 times stronger than the reflected shortwave radiation by cloud, while the contribution of water vapour to shortwave radiation is almost negligible. The longwave radiation ~~change~~anomalies in response to cloud and water vapour is attributed to downwelling longwave radiation, as upwelling longwave radiation depends solely on the surface temperature according to the Stefan–Boltzmann law, and its seasonal variation is relatively small compared to the significant seasonality ~~showing~~ in shortwave radiation. The Pliocene sea -ice decline ~~accelerates~~, as compared to the preindustrial period, amplifies the turbulent exchange between the ocean and atmosphere, and the annual sum of sensible and latent heat ~~fluxes exceed~~flux anomalies exceeds radiation ~~fluxes.~~flux anomalies. In particular, heat is released to the atmosphere by the prominent enhanced turbulent heat ~~fluxes~~flux anomalies in ~~winter, amplifying the atmospheric warming~~November, contributing to the formation of the maximum SAT anomaly in November.

A synthesis of Arctic amplification given by Serreze and Barry (2011) has introduced some of the physical processes mentioned above, including sea ice loss, albedo feedback, cloud cover, and water vapour. Unlike Serreze and Barry (2011), in this work we apply CFRAM and an EFA-like method to untangle these physical processes and obtain a quantitative understanding of sea-ice effects, which would help to directly evaluate the impact on heat exchange once the sea-ice concentration variation within Arctic is given. The EC-Earth simulation shows a stronger Arctic amplification than multi-model ensembles (Dowsett et al., 2012). However, an underestimation of Arctic warming as compared to proxy data remains in the EC-Earth simulation, implying less warmth produced by the EC-Earth model from oceanic heat transport, which yields a clue for improving the simulation. Furthermore, caution should be exercised when discussing sea-ice effects on heat flux, as underestimating Arctic warming might affect the interface heat exchange.

Though significant albedo and insulation effects of sea -ice have been studied, the possible nonlinear response of heat flux to sea -ice can not be captured in this work. In addition, ~~the~~ this approach to ~~extract~~extracting sea -ice effects is based on ~~the~~ spatial correlation~~,~~; whether the corresponding conclusion is consistent with that from EFA ~~method~~ remains uncertain. The consistency check is computationally expensive for CFRAM calculation, as ~~the~~ EFA requires high temporal resolution. The present study is based on the Pliocene simulation with the EC-Earth, and the results may be model -dependent. Further work is needed to compare our results with other PlioMIP models.

Acknowledgements. This work was supported by the Swedish Research Council VR for the Swedish~~-~~–French project GIWA, the China Scholarship Council (Grant 201606345010~~)~~), and the Opening Project of Key Laboratory of Meteorological Disaster of Ministry of Education of Nanjing University of Information Science and Technology (Grant KLME1401). The EC-Earth mid-Pliocene simulation ~~is~~was performed at ECMWF's computing and archive facilities, and the analysis ~~are~~was performed on resources provided by the Swedish National Infrastructure for Computing (SNIC) at Linköping University.

References

Alexander, M.A., Bhatt, U.S., Walsh, J.E., Timlin, M.S., Miller, J.S. and Scott, J.D.: The atmospheric response to realistic Arctic sea ice anomalies in an AGCM during winter, J. Climate, 17, 890-905, doi:10.1175/1520-0442(2004)017<0890:TARTRA>2.0.CO;2, 2004.

Alexeev, V.A., Ivanov, V.V., Kwok, R. and Smedsrud, L.H.: North Atlantic warming and declining volume of arctic sea ice, The Cryosphere Discussions, 7, 245-265, doi:10.5194/tcd-7-245-2013, 2013.

Ballantyne, A.P., Axford, Y., Miller, G.H., Otto-Bliesner, B.L., Rosenbloom, N. and White, J.W.: The amplification of Arctic terrestrial surface temperatures by reduced sea-ice extent during the Pliocene, Palaeogeogr. Palaeoclimatol. Palaeoecol., 386, 59-67, doi:10.1016/j.palaeo.2013.05.002, 2013.

Balsamo, G., Beljaars, A., Scipal, K., Viterbo, P., van den Hurk, B., Hirschi, M. and Betts, A.K.: A revised hydrology for the ECMWF model: Verification from field site to terrestrial water storage and impact in the Integrated Forecast System, J. Hydrometeorol., 10, 623-643, doi:10.1175/2008JHM1068.1, 2009.

Bintanja, R. and Selten, F.M.: Future increases in Arctic precipitation linked to local evaporation and sea-ice retreat, Nature, 509, 479-482, doi:10.1038/nature13259, 2014.

Bretherton, C.S., Widmann, M., Dymnikov, V.P., Wallace, J.M. and Bladé, I.: The effective number of spatial degrees of freedom of a time-varying field, J. Climate, 12, 1990-2009, doi:10.1175/1520-0442(1999)012<1990:TENOSD>2.0.CO;2, 1999.

Brierley, C. M. and Fedorov, A. V.: Comparing the impacts of Miocene–Pliocene changes in inter-ocean gateways on climate: Central American Seaway, Bering Strait, and Indonesia, Earth Planet. Sci. Lett., 444, 116-130, doi:10.1016/j.epsl.2016.03.010, 2016.

Brigham-Grette, J., Melles, M., Minyuk, P., Andreev, A., Tarasov, P., DeConto, R. and Haltia, E.: Pliocene warmth, polar amplification, and stepped Pleistocene cooling recorded in NE Arctic Russia. Science, 340, 1421, doi:10.1126/science.1233137, 2013.

Burt, M.A., Randall, D.A. and Branson, M.D.: Dark warming, J. Climate, 29, 705-719, doi:10.1175/JCLI-D-15-0147.1, 2016.

Dowsett, H.J., Robinson, M.M., Haywood, A.M., Hill, D.J., Dolan, A.M., Stoll, D.K., Abe-Ouchi, A., Chandler, M.A., Rosenbloom, N.A., Otto-Bliesner, B.L. and Bragg, F.J.: Assessing confidence in Pliocene sea surface temperatures to evaluate predictive models, Nat. Clim. Change, 2, 365-371, doi:10.1038/nclimate1455, 2012.

Dowsett, H., Dolan, A., Rowley, D., Moucha, R., Forte, A. M., Mitrovica, J. X., Pound, M., Salzmann, U., Robinson, M., Chandler, M., Foley, K., and Haywood, A.: The PRISM4 (mid-Piacenzian) paleoenvironmental reconstruction, Clim. Past, 12, 1519-1538, doi:10.5194/cp-12-1519-2016, 2016.

Fedorov, A.V., Dekens, P.S., McCarthy, M., Ravelo, A.C., Barreiro, M., Pacanowski, R.C. and Philander, S.G.: The Pliocene paradox (mechanisms for a permanent El Niño), Science, 312, 1485-1489, doi:10.1126/science.1122666, 2006.

Feng, R., Otto-Bliesner, B. L., Fletcher, T. L., Tabor, C. R., Ballantyne, A. P., & Brady, E. C.: Amplified Late Pliocene terrestrial warmth in northern high latitudes from greater radiative forcing and closed Arctic Ocean gateways, Earth Planet. Sci. Lett., 466, 129-138, doi:10.1016/j.epsl.2017.03.006, 2017.

Frankignoul, C. and Kestenare, E.: The surface heat flux feedback. Part I: estimates from observations in the Atlantic and the North Pacific, Clim. Dynam., 19, 633-647, doi:10.1007/s00382-002-0252-x, 2002.

Fu, Q. and Liou, K.N.: Parameterization of the radiative properties of cirrus clouds, J. Atmos. Sci., 50, 2008–2025, doi:10.1175/1520-0469(1993)050<2008:POTRPO>2.0.CO;2, 1993.

Gaetani, M., Messori G., Zhang Q., Flamant C., and Pausata F.S.: Understanding the mechanisms behind the northward extension of the West African Monsoon during the Mid-Holocene. J. Climate, doi:10.1175/JCLI-D-16-0299.1, 2017.

Gildor, H., Ashkenazy, Y., Tziperman, E. and Lev, I.: The role of sea ice in the temperature-precipitation feedback of glacial cycles, Clim. Dynam., 43, 1001-1010, doi:10.1007/s00382-013-1990-7, 2014.

Graversen, R.G. and Burtu, M.: Arctic amplification enhanced by latent energy transport of atmospheric planetary waves, Q. J. Roy. Meteor. Soc., 142, 2046-2054, doi:10.1002/qj.2802, 2016.

Haywood, A.M., Dowsett, H.J. and Dolan, A.M.: Integrating geological archives and climate models for the mid-Pliocene warm period, Nat. Commun., 7, 1-14, doi:10.1038/ncomms10646, 2016a.

Haywood, A.M., Dowsett, H.J., Dolan, A.M., Chandler, M.A., Hunter, S.J. and Lunt, D.J.: The Pliocene Model

Intercomparison Project (PlioMIP) Phase 2: scientific objectives and experimental design, Clim. Past, 12, 663-675, doi:10.5194/cp-12-663-2016, 2016b.

Hazeleger, W., Wang, X., Severijns, C., Ştefănescu, S., Bintanja, R., Sterl, A., Wyser, K., Semmler, T., Yang, S., Van den Hurk, B. and Van Noije, T.: EC-Earth V2. 2: description and validation of a new seamless earth system prediction model, Clim. Dynam., 39, 2611-2629, doi:10.1007/s00382-011-1228-5, 2012.

Hill, D.J., Haywood, A.M., Lunt, D.J., Hunter, S.J., Bragg, F.J., Contoux, C., Stepanek, C., Sohl, L., Rosenbloom, N.A., Chan, W.L. and Kamae, Y.: Evaluating the dominant components of warming in Pliocene climate simulations, Clim. Past, 10, 79-90, doi:10.5194/cp-10-79-2014, 2014.

Hu, X., Li, Y., Yang, S., Deng, Y. and Cai, M.: Process-based Decomposition of the Decadal Climate Difference between 2002-13 and 1984-95, J. Climate, 30, 4373-4393, doi:10.1175/JCLI-D-15-0742.1, 2017.

Kageyama, M., Braconnot, P., Harrison, S. P., Haywood, A. M., Jungclaus, J. H., Otto-Bliesner, B. L., Peterschmitt, J.-Y., Abe-Ouchi, A., Albani, S., Bartlein, P. J., Brierley, C., Crucifix, M., Dolan, A., Fernandez-Donado, L., Fischer, H., Hopcroft, P. O., Ivanovic, R. F., Lambert, F., Lunt, D. J., Mahowald, N. M., Peltier, W. R., Phipps, S. J., Roche, D. M., Schmidt, G. A., Tarasov, L., Valdes, P. J., Zhang, Q., and Zhou, T.: The PMIP4 contribution to CMIP6 – Part 1: Overview and over-arching analysis plan, Geosci. Model Dev., 11(3), 1033-1057, doi:10.5194/gmd-11-1033-2018, 2018.

Kim, K.Y., Hamlington, B.D., Na, H. and Kim, J.: Mechanism of seasonal Arctic sea ice evolution and Arctic amplification, The Cryosphere, 10(5), 2191-2202, doi:10.5194/tc-10-2191-2016, 2016.

Koenigk, T., Brodeau, L., Graversen, R. G., Karlsson, J., Svensson, G., Tjernström, M. and Wyser, K.: Arctic climate change in 21st century CMIP5 simulations with EC-Earth, Climate dynamics, 40(11-12), 2719-2743, doi: 10.1007/s00382-012-1505-y, 2013.

Krumpen, T., Gerdes, R., Haas, C., Hendricks, S., Herber, A., Selyuzhenok, V., Smedsrud, L. and Spreen, G.: Recent summer sea ice thickness surveys in Fram Strait and associated ice volume fluxes, The Cryosphere, 10, 523-534, doi:10.5194/tc-10-523-2016, 2016.

Lang, A., Yang, S. and Kaas, E.: Sea-ice thickness and recent Arctic warming, Geophys. Res. Lett., 44, 409-418, doi:10.1002/2016GL071274, 2017.

Li, C., Notz, D., Tietsche, S. and Marotzke, J.: The transient versus the equilibrium response of sea ice to global warming, J.Climate, 26, 5624-5636, doi:10.1175/JCLI-D-12-00492.1, 2013.

Li, G., Ren, B., Zheng, J. and Yang, C.: Net air–sea surface heat flux during 1984–2004 over the North Pacific and North Atlantic oceans (10N–50N): annual mean climatology and trend, Theor. Appl. Climatol., 104, 387-401, doi: 10.1007/s00704-010-0351-2, 2011.

Liu, Y., Key, J.R., Liu, Z., Wang, X. and Vavrus, S.J.: A cloudier Arctic expected with diminishing sea ice, Geophys. Res. Lett., 39, L05705, doi:10.1029/2012GL051251, 2012.

Lu, J. and Cai, M.: A new framework for isolating individual feedback processes in coupled general circulation climate models. Part I: Formulation, Clim. Dynam., 32, 873–885, doi:10.1007/s00382-008-0425-3, 2009.

Madec, G.: ‘‘NEMO ocean engine’’. Note du Pole de mode ́lisation, Institut Pierre-Simon Laplace (IPSL), France, No 27 ISSN no 1288-1619, 2008.

Matthiessen, J., Knies, J., Vogt, C. and Stein, R.: Pliocene palaeoceanography of the Arctic Ocean and subarctic seas, Philos. Trans. R. Soc. A., 367, 21–48, doi: 10.1098/rsta.2008.0203, 2009.

Muschitiello, F., Zhang, Q., Sundqvist, H.S., Davies, F.J. and Renssen, H.: Arctic climate response to the termination of the African Humid Period, Quat. Sci. Rev., 125, 91-97, doi:10.1016/j.quascirev.2015.08.012, 2015.

Nghiem, S.V., Rigor, I.G., Perovich, D.K., Clemente-Colón, P., Weatherly, J.W. and Neumann, G.: Rapid reduction of Arctic perennial sea ice, Geophys. Res. Lett., 34, L19504, doi:10.1029/2007GL031138, 2007.

Otto-Bliesner, B. L., Jahn, A., Feng, R., Brady, E. C., Hu, A., and Löfverström, M.: Amplified North Atlantic warming in the late Pliocene by changes in Arctic gateways, Geophys. Res. Lett., *44*(2), 957-964, doi:10.1002/2016GL071805, 2017.

Overland J.E., Wang M., Walsh J.E., Christensen J.H., Kattsov V.M., Champan W.L.: Climate model projections for the Arctic. In: AMAP (2011) Snow, Water, Ice and Permafrost in the Arctic (SWIPA): Climate Change and the Cryosphere. Arctic Monitoring and Assessment Programme (AMAP), Oslo, Norway. Xii, 538 pp , 2011.

Pausata, F.S., Messori, G. and Zhang, Q.: Impacts of dust reduction on the northward expansion of the African monsoon during the Green Sahara period, Earth Planet. Sci. Lett., 434, 298-307, doi:10.1016/j.epsl.2015.11.049, 2016.

Pausata, F.S., Emanuel, K.A., Chiacchio, M., Diro, G.T., Zhang, Q., Sushama, L., Stager, J.C. and Donnelly, J.P.: Tropical cyclone activity enhanced by Sahara greening and reduced dust emissions during the African Humid Period, Proc. Natl. Acad. Sci., 114, 6221-6226, doi:10.1073/pnas.1619111114, 2017a.

Pausata, F.S., Zhang, Q., Muschitiello, F., Lu, Z., Chafik, L., Niedermeyer, E.M., Stager, J.C., Cobb, K.M. and Liu, Z.: Greening of the Sahara suppressed ENSO activity during the mid-Holocene, Nat. Commun., *8*, 1-12, doi:10.1038/ncomms16020, 2017b.

Pithan, F. and Mauritsen, T.: Arctic amplification dominated by temperature feedbacks in contemporary climate models, Nat. Geosci., 7, 181-184, doi:10.1038/ngeo2071, 2014.

Robinson, M.M., Dowsett, H.J. and Chandler, M.A.: Pliocene role in assessing future climate impacts, EOS, Trans. Am. Geophys. Union, 89, 501-502, doi:10.1029/2008EO490001, 2008.

Serreze, M.C., Barrett, A.P., Stroeve, J.C., Kindig, D.N. and Holland, M.M.: The emergence of surface-based Arctic amplification, The Cryosphere, 3, 11-19, doi:10.5194/tc-3-11-2009, 2009.

Serreze, M.C. and Barry, R.G.: Processes and impacts of Arctic amplification: A research synthesis, Glob. Planet. Chang., 77, 85-96, doi:10.1016/j.gloplacha.2011.03.004, 2011.

Sévellec, F., Fedorov, A.V. and Liu, W.: Arctic sea-ice decline weakens the Atlantic Meridional Overturning Circulation, Nat. Clim. Change, 7, 604-610, doi:10.1038/nclimate3353, 2017.

Shine, K.P. and Henderson-Sellers, A.: The sensitivity of a thermodynamic sea ice model to changes in surface albedo parameterization. Journal of Geophysical Research, 90, 2243–2250, 1985.

Soden, B. J. and Held, I. M.: An assessment of climate feedbacks in coupled ocean–atmosphere models, J. Climate, 19, 3354–3360, doi:10.1175/JCLI3799.1., 2006.

Song, X. and Zhang, G.J.: Role of climate feedback in El Niño–like SST response to global warming, J. Climate, *27*, 7301-7318, doi:10.1175/JCLI-D-14-00072.1, 2014.

Taylor, P.C., Cai, M., Hu, A., Meehl, J., Washington, W. and Zhang, G.J.: A decomposition of feedback contributions to polar warming amplification. J. Climate, 26, 7023-7043, doi:10.1175/JCLI-D-12-00696.1, 2013.

Valcke, S.: OASIS3 user guide (prism_2-5), PRISM report series, no 2, 6th edn., 2006.

Vancoppenolle, M., Fichefet T., Goosse H., Bouillon S., Madec G. and Maqueda M. A.: Simulating the mass balance and salinity of Arctic and Antarctic sea ice. 1. Model description and validation, Ocean Modelling, 27, 33-53, doi:10.1016/j.oceamod.2008.10.005., 2009.

Venegas, S. A., Mysak, L. A. and Straub, D. N.: Atmosphere–ocean coupled variability in the South Atlantic. J. Climate, 10(11), 2904-2920, doi:10.1175/1520-0442(1997)010<2904:AOCVIT>2.0.CO;2, 1997.

Vihma, T.: Effects of Arctic sea ice decline on weather and climate: a review. Surv. Geophys., 35, 1175-1214, doi:10.1007/s10712-014-9284-0, 2014.

Wara, M.W., Ravelo, A.C. and Delaney, M.L.: Permanent El Niño-like conditions during the Pliocene warm period. Science, 309, 758-761, doi:10.1126/science.1112596, 2005.

Wetherald, R. T. and Manabe S.: Cloud feedback processes in a general circulation model. J. Atmos. Sci., 45, 1397–1416, doi:10.1175/1520-0469(1988)045,1397:CFPIAG.2.0.CO;2., 1988.

Winton, M.: Sea ice–albedo feedback and nonlinear Arctic climate change. Arctic sea ice decline: Observations, projections, mechanisms, and implications, 111-131, doi:10.1029/180GM09, 2008.

Zheng, J., Ren, B., Li, G. and Yang, C.: Seasonal dependence of local air-sea interaction over the tropical Western Pacific warm pool. J. Trop. Meteorol., 20(4), 360-367, doi:10.16555/j.1006-8775.2014.04.009, 2014.

Table 1. The spatial standard deviation of SIC anomalies σ_{SIC} and net shortwave radiation anomalies due to albedo effect $\sigma_{SW\text{-}albedo}$ (Wm^{-2}) over the Arctic Ocean. $r_{SW\text{-}albedo}$ is the correlation coefficient between SIC and shortwave radiation anomalies. Those significant at a 99% confidence level are bolded.

	Jan	Feb	Mar	Apr	May	Jun	Jul	Aug	Sep	Oct	Nov	Dec
σ_{SIC}	0.~~44~~25	0.~~44~~26	0.~~44~~26	0.~~43~~26	0.~~43~~25	0.~~39~~23	0.~~34~~23	0.~~36~~20	0.~~39~~19	0.~~38~~25	0.~~40~~25	0.~~43~~25
$\sigma_{SW\text{-}albedo}$	0.~~03~~01	~~1.55~~0.75	~~11.09~~5.81	~~42.79~~25.34	~~88.43~~52.45	~~80.37~~48.79	~~41.88~~26.28	~~29.85~~12.39	~~15.06~~6.85	~~3.59~~2.16	0.~~20~~21	0
$r_{SW\text{-}albedo}$	~~-~~–0.~~25~~22	~~-~~–0.~~43~~37	**~~-~~–0.~~75~~63**	**~~-~~–0.~~88~~77**	**~~-~~–0.~~90~~80**	**~~-~~–0.~~91~~85**	**~~-~~–0.~~90~~85**	**~~-~~–0.~~93~~83**	**~~-~~–0.~~88~~57**	**~~-~~–0.~~50~~53**	~~-~~–0.~~25~~11	/

Table 2. The spatial standard deviation of shortwave and longwave radiation anomalies due to cloud change ($\sigma_{SW\text{-}cloud}$, $\sigma_{LW\text{-}cloud}$) (Wm^{-2}) and water vapour change ($\sigma_{SW\text{-}WV}$, $\sigma_{LW\text{-}WV}$) (Wm^{-2}) over the Arctic Ocean. $r_{SW\text{-}cloud}$, $r_{LW\text{-}cloud}$, $r_{SW\text{-}WV}$, and $r_{LW\text{-}WV}$ are correlation coefficients between SIC and shortwave and longwave radiation anomalies due to cloud and water change, respectively. Those significant at a 99% confidence level are bolded. Here, the cloud and water vapour change is specified as the part caused by sea -ice decrease.

	Annual	Jan	Feb	Mar	Apr	May	Jun	Jul	Aug	Sep	Oct	Nov	Dec
$\sigma_{SW\text{-}cloud}$	4.76	0.01	0.16	1.11	3.86	5.97	11.71	19.61	13.86	3.21	0.50	0.04	0
$r_{SW\text{-}cloud}$	0.18	0.14	0.22	0.36	0.36	0.16	0.01	0.05	0.24	0.26	0.25	0.32	/
$\sigma_{LW\text{-}cloud}$	8.02	9.13	9.29	8.25	7.64	10.20	11.91	15.11	13.56	11.96	10.01	10.18	9.86
$r_{LW\text{-}cloud}$	**–0.46**	**–0.59**	**–0.56**	**–0.56**	**–0.51**	–0.36	0.06	0.04	–0.23	**–0.54**	**–0.41**	**–0.60**	**–0.56**
$\sigma_{SW\text{-}WV}$	0.29	0.001	0.03	0.14	0.40	0.59	0.85	0.85	0.63	0.33	0.09	0.01	0
$r_{SW\text{-}WV}$	–0.02	–0.05	0.02	0.06	0.05	0.02	0.11	–0.07	**–0.57**	**–0.62**	**–0.43**	–0.22	/
$\sigma_{LW\text{-}WV}$	2.27	3.45	3.53	3.11	2.84	2.57	2.72	2.15	1.73	1.77	2.31	2.89	3.54
$r_{LW\text{-}WV}$	**–0.56**	**–0.45**	**–0.43**	**–0.50**	**–0.58**	**–0.57**	**–0.46**	–0.13	0.38	0.13	–0.36	**–0.58**	**–0.49**

	~~Annual~~	~~Jan~~	~~Feb~~	~~Mar~~	~~Apr~~	~~May~~	~~Jun~~	~~Jul~~	~~Aug~~	~~Sep~~	~~Oct~~	~~Nov~~	~~Dec~~
~~$\sigma_{SW\text{-}cloud}$~~	**~~4.86~~76**	**~~0.01~~**	**~~0.16~~**	**~~1.20~~11**	**~~4.56~~3.86**	**~~6.84~~5.97**	**~~12.53~~11.71**	**~~19.14~~61**	**~~14.45~~13.86**	**~~4.16~~3.21**	**~~0.65~~50**	**~~0.04~~**	**~~0~~**
~~$r_{SW\text{-}cloud}$~~	**~~0.31~~18**	**~~0.15~~14**	**~~0.27~~22**	**~~0.41~~36**	**~~0.42~~36**	**~~0.29~~16**	**~~0.19~~01**	**~~0.21~~05**	**~~0.35~~24**	**~~0.40~~26**	**~~0.37~~25**	**~~0.32~~**	**~~/~~**

$\sigma_{LW-cloud}$	8.2502	8.899.13	9.1929	8.1325	7.9664	10.7320	11.8191	14.0615.11	13.5556	13.6411.96	11.3110.01	10.3118	9.8386
$r_{LW-cloud}$	–0.5246	–0.5859	–0.5956	–0.5856	–0.5551	–0.4536	-0.0906	-0.0704	–0.3323	–0.6254	–0.5241	–0.6460	–0.5856
σ_{SW-WV}	0.2729	0.001	0.03	0.14	0.3840	0.5759	0.7985	0.7785	0.5663	0.2833	0.0809	0.01	0
r_{SW-WV}	–0.0702	–0.0805	-0.0302	0.0106	-0.0105	-0.0602	0.0611	–0.0807	–0.4957	–0.5662	–0.4443	–0.2422	/
σ_{LW-WV}	2.2327	3.4045	3.4653	3.0711	2.8084	2.5157	2.5372	1.922.15	1.5573	1.5877	2.2131	2.9689	3.6154
r_{LW-WV}	–0.6256	–0.5045	–0.4843	–0.5650	–0.6258	–0.6057	–0.4846	–0.1213	0.3338	-0.0613	–0.5236	–0.6758	–0.5749

Table 3. The spatial standard deviation of sensible and latent heat flux anomalies σ_{SH}, σ_{LH} (Wm^{-2}) over the Arctic Ocean. r_{SH} and r_{LH} are correlation coefficients between SIC and sensible and latent heat flux anomalies, respectively. Those significant at a 99% confidence level are bolded.

	Jan	Feb	Mar	Apr	May	Jun	Jul	Aug	Sep	Oct	Nov	Dec
σ_{SH}	28.53	29.44	21.64	12.87	7.94	9.46	9.55	2.63	2.11	7.02	31.11	26.80
r_{SH}	**0.57**	**0.64**	**0.67**	**0.66**	**0.76**	0.26	–0.36	0.03	**0.65**	**0.80**	**0.71**	**0.56**
σ_{LH}	18.70	19.00	14.75	9.46	5.64	5.84	8.75	1.93	1.69	5.77	19.87	17.44
r_{LH}	**0.74**	**0.77**	**0.78**	**0.76**	**0.71**	0.14	**–0.42**	–0.37	**0.69**	**0.90**	**0.79**	**0.72**

Table 4. The response coefficients (Wm^{-2}) of radiation and turbulent heat fluxes to the albedo and insulation effects of sea ~~-~~ice. Those significant at a 99% confidence level are bolded.

λ (Wm^{-2})	flux		Ann	Jan	Feb	Mar	Apr	May	Jun	Jul	Aug	Sep	Oct	Nov	Dec
albedo	SW		**~~-46.5~~–43.0**	0.0	~~-~~–1.~~7~~1	**~~-18.9~~–13.8**	**~~-87.2~~–75.0**	**~~-188.1~~–169.2**	**~~-186.0~~–178.3**	**~~-109.7~~–97.0**	**~~-77.5~~–52.0**	**~~-34.4~~–20.2**	~~-~~–**4.~~7~~5**	~~-~~–0.1	0
insulation	SW	cloud	~~4.3~~2.6	0.0	0.1	~~1.1~~0.9	~~4.4~~3.1	~~4.6~~2.3	~~6.1~~0.4	~~11.~~3.1	~~13.7~~9.6	~~4.~~2.3	0.~~6~~4	0.0	0
		WV	~~-~~–0.~~1~~0	0.0	0.0	0.0	0.0	~~-~~0.~~1~~0	0.~~1~~2	~~-~~–0.2	~~-~~**–1.0**~~.7~~	~~-~~–**0.~~4~~5**	~~-~~–0.1	0.0	0
	LW	cloud	**~~-12.6~~–11.1**	**~~-11.9~~–12.1**	**~~-12.2~~–11.7**	~~-~~–**10.~~8~~4**	**~~-10.0~~–8.9**	~~**-11.4**~~–8.6	~~-2~~1.7	~~-2.8~~1.9	~~-12.2~~–9.0	**~~-21.3~~–17.6**	**~~-15.2~~–11.6**	**~~-16.4~~–15.8**	~~-~~–**13.~~6~~0**
		WV	**~~-4.0~~–3.9**	~~-~~–**3.~~9~~5**	~~-~~–**3.~~8~~4**	~~-~~–**3.~~9~~5**	**~~-4.0~~–3.7**	~~-~~–**3.~~6~~4**	~~-~~–**3.~~1~~2**	~~-~~–0.~~7~~9	1.~~4~~9	~~-~~0.~~3~~6	~~-~~–2.3~~.0~~	**~~-5.0~~–4.4**	~~-~~–**4.~~8~~1**
	SH		**35.3**	**53.4**	**59.0**	**46.4**	**29.6**	**24.2**	10.4	~~-~~–13.8	0.4	**7.1**	**22.3**	**79.2**	**54.0**
	LH		**27.7**	**45.3**	**46.0**	**36.6**	**25.0**	**16.1**	3.5	~~-~~**–15.0**	~~-~~–3.6	**6.0**	**20.5**	**56.7**	**45.7**

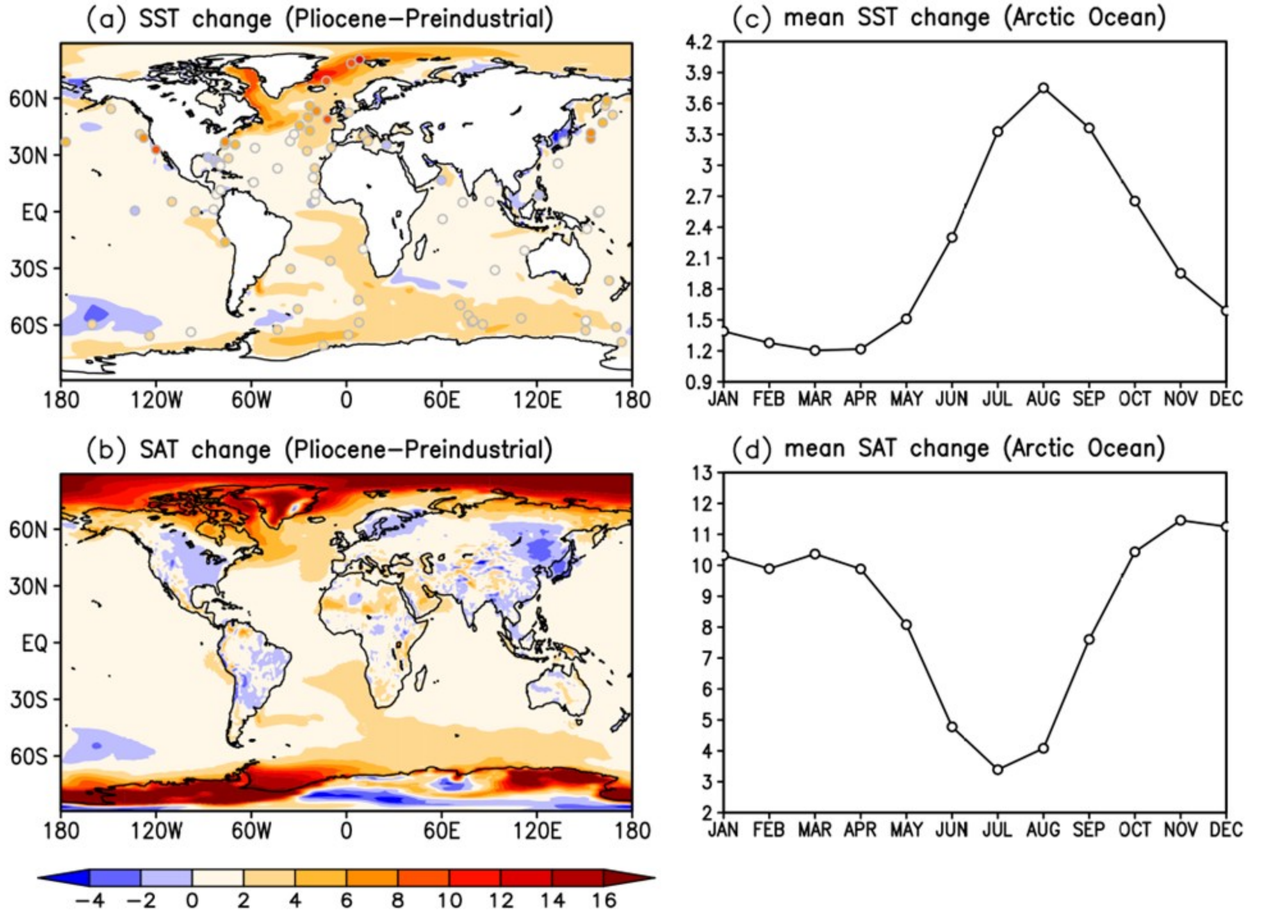
(a) SST change (Pliocene–Preindustrial)
(b) SAT change (Pliocene–Preindustrial)
(c) mean SST change (Arctic Ocean)
(d) mean SAT change (Arctic Ocean)
60N
30N
EQ
30S
60S
180
120W
60W
0
60E
120E
180
−4 −2 0 2 4 6 8 10 12 14 16
4.2 3.9 3.6 3.3 3 2.7 2.4 2.1 1.8 1.5 1.2 0.9
13 12 11 10 9 8 7 6 5 4 3 2
JAN FEB MAR APR MAY JUN JUL AUG SEP OCT NOV DEC

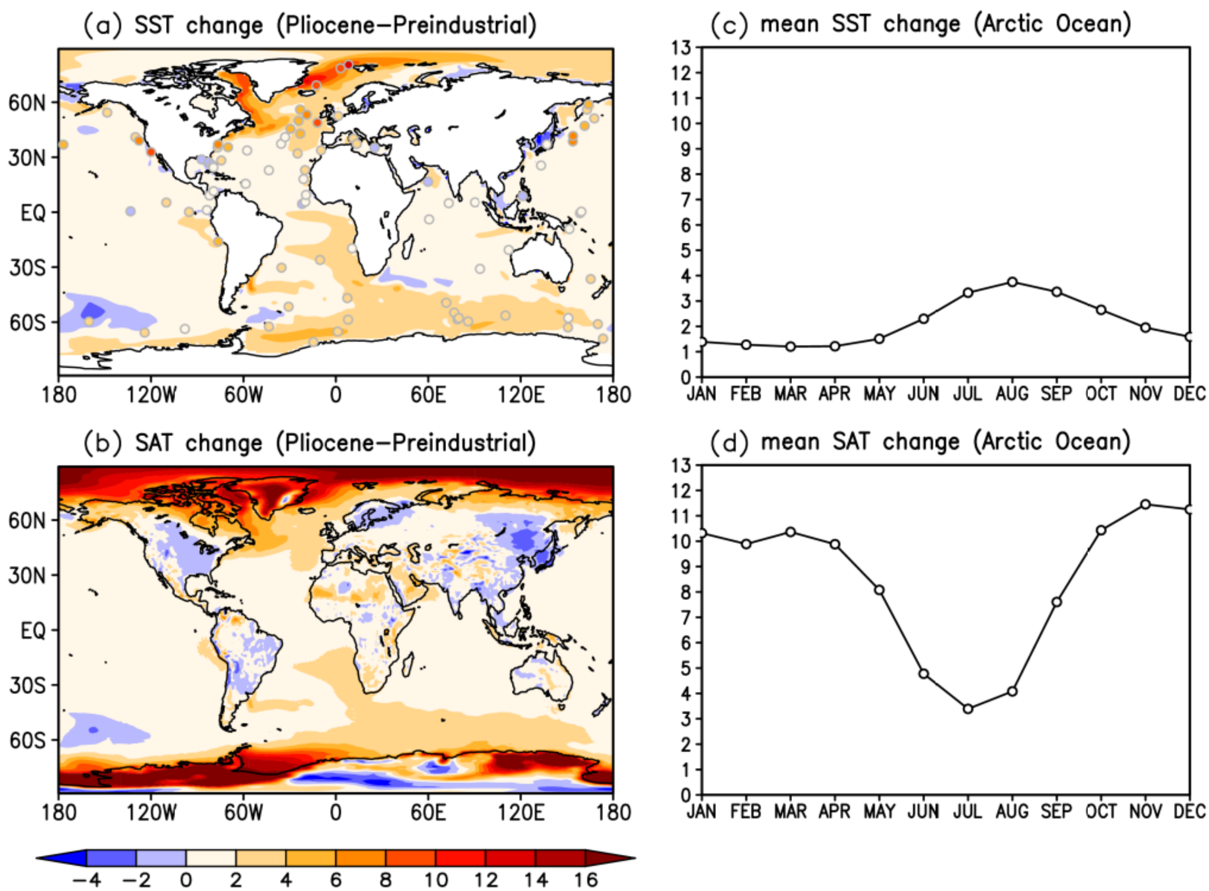

Figure 1. The annual mean warming (K) for (a) sea surface temperature (SST~~),~~) and (b) surface air temperature (SAT~~)~~), and seasonal warming (K) averaged over the Arctic Ocean for (c) SST~~,~~ and (d) SAT between the Pliocene and preindustrial simulations. The shaded circles in (a) represent the annual mean SST anomalies at 95% confidence-assessed marine sites from the Deep Sea Drilling Project (DSDP) and Ocean Drilling Program (ODP).

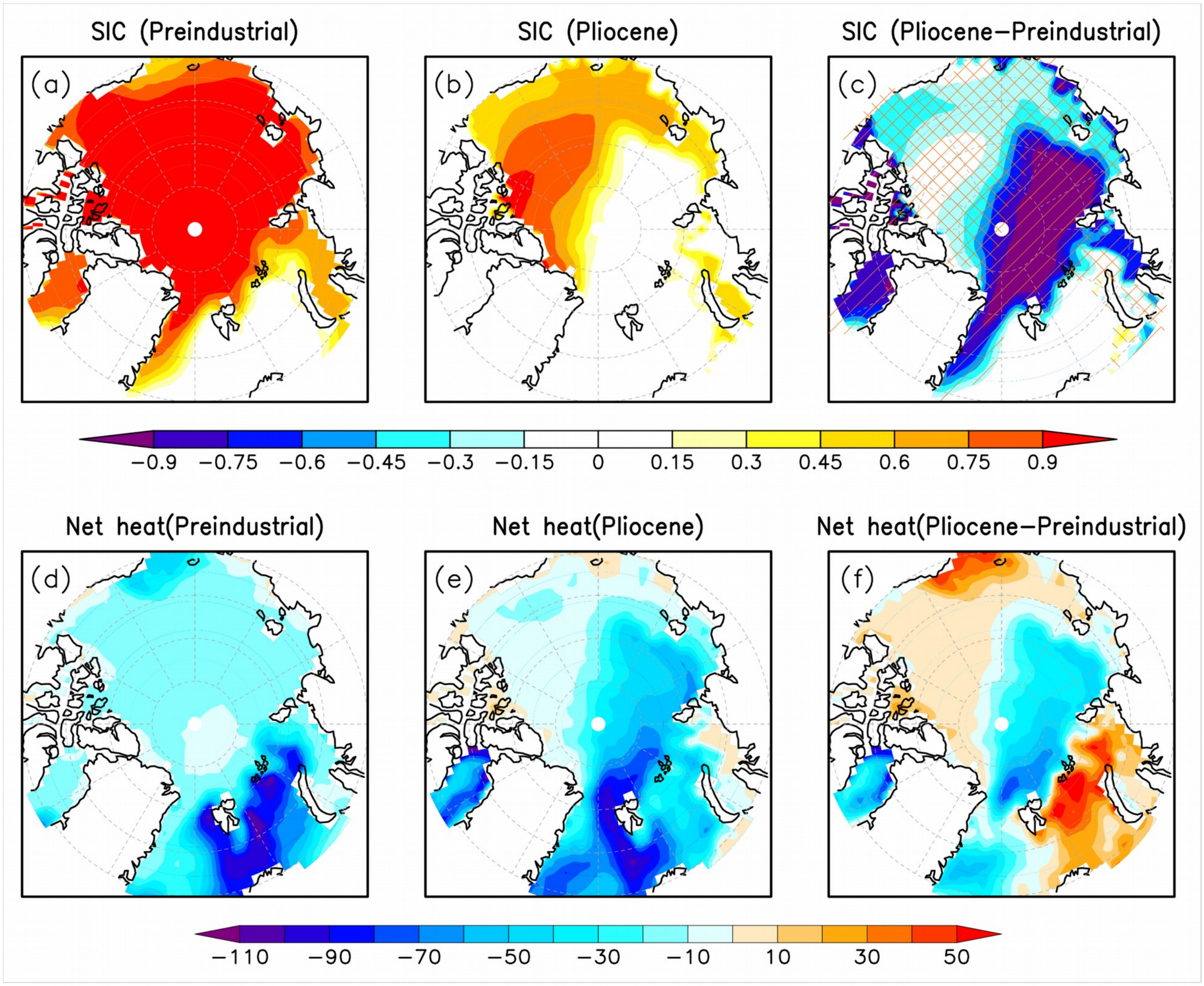
SIC (Preindustrial)
SIC (Pliocene)
SIC (Pliocene−Preindustrial)
(a)
(b)
(c)
−0.9 −0.75 −0.6 −0.45 −0.3 −0.15 0 0.15 0.3 0.45 0.6 0.75 0.9
Net heat(Preindustrial)
Net heat(Pliocene)
Net heat(Pliocene−Preindustrial)
(d)
(e)
(f)
−110 −90 −70 −50 −30 −10 10 30 50

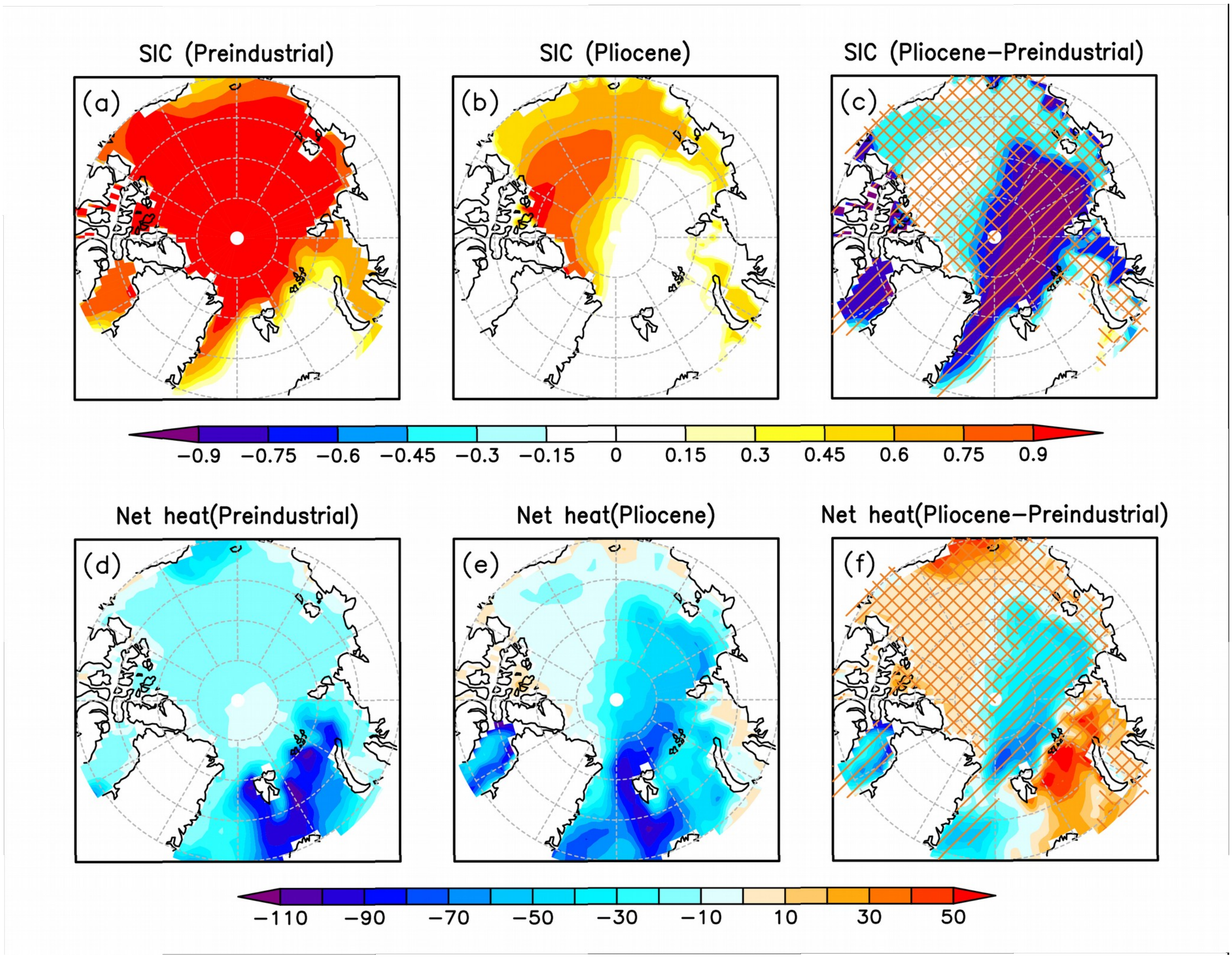

Figure 2. Spatial distributions of the annual mean sea ~~-~~ice concentration (SIC) and ~~air-sea interface~~ net heat flux at the surface of ice and ocean (Wm^{-2}, positive downward) over the Arctic Ocean. (a) SIC in the preindustrial period, (b) SIC in the Pliocene, (c) the Pliocene SIC change with respect to the preindustrial period, (d) net heat flux in the preindustrial period, (e) net heat flux in the Pliocene, and (f) the Pliocene net heat flux change with respect to the preindustrial period. The diagonal stripe in (c) represents the regions from ice-covered to ice-free, and the diagonal crosshatch represents the regions from ice-covered to ice-covered.

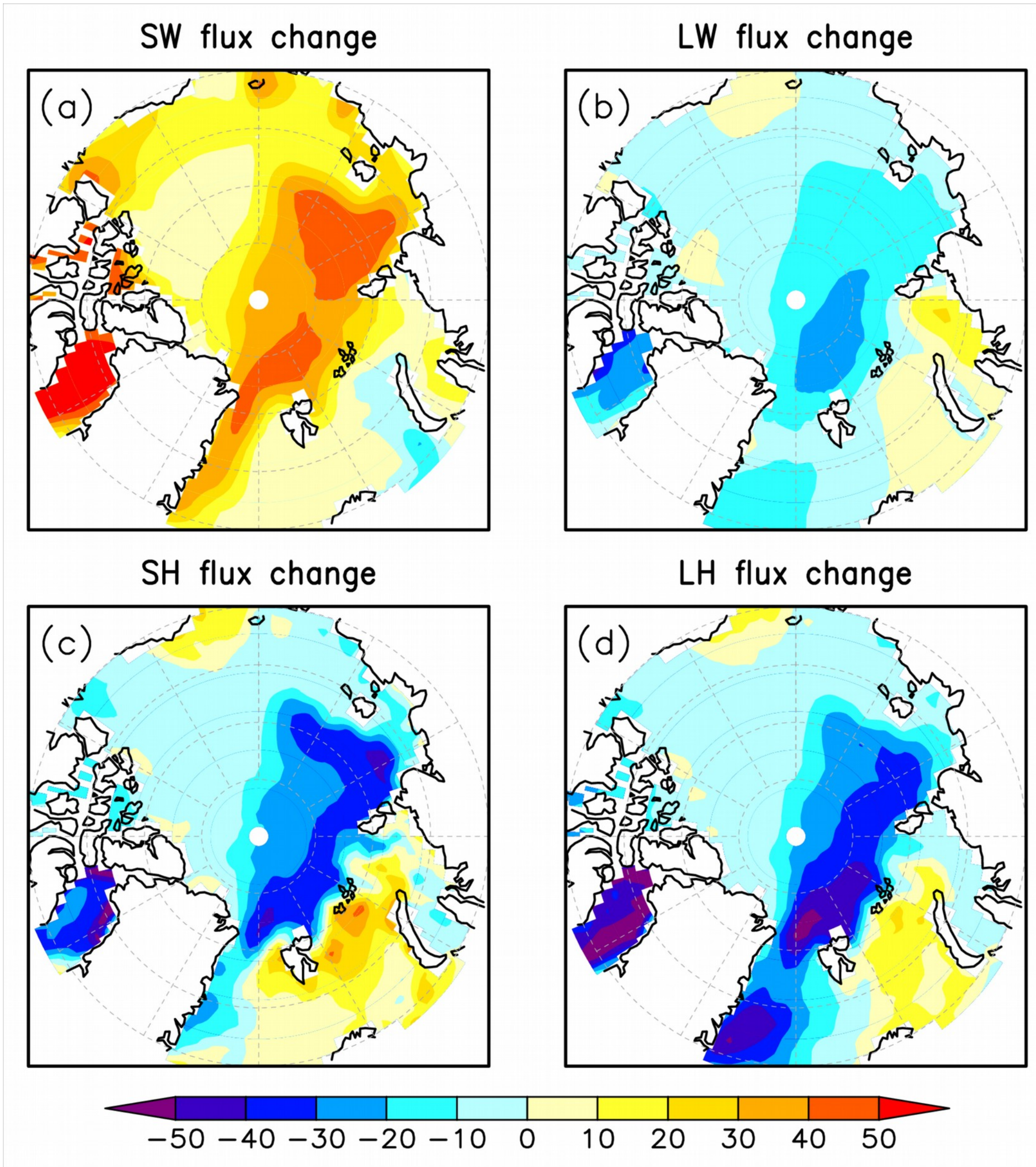

Figure 3. Spatial distributions of the Pliocene annual mean heat flux change (Wm^{-2}, positive downward) with respect to the preindustrial period over the Arctic Ocean. (a) net shortwave ~~radiation~~ flux, (b) net longwave radiation flux, (c) sensible heat flux, and (d) latent heat flux.

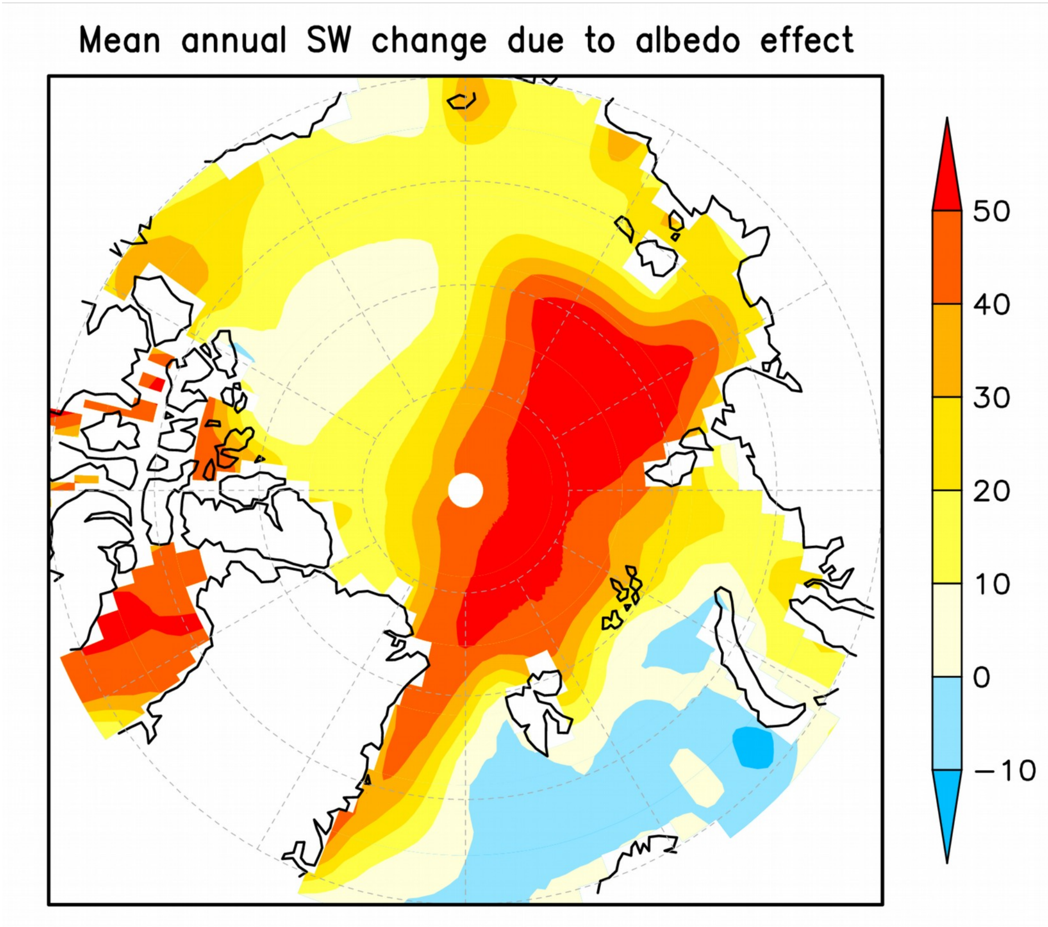

Figure 4. Spatial distributions of the Pliocene annual mean net shortwave ~~radiation~~ flux change (Wm^{-2}, positive downward) at the surface over the Arctic Ocean caused by albedo effect of sea -ice change with respect to the preindustrial period.

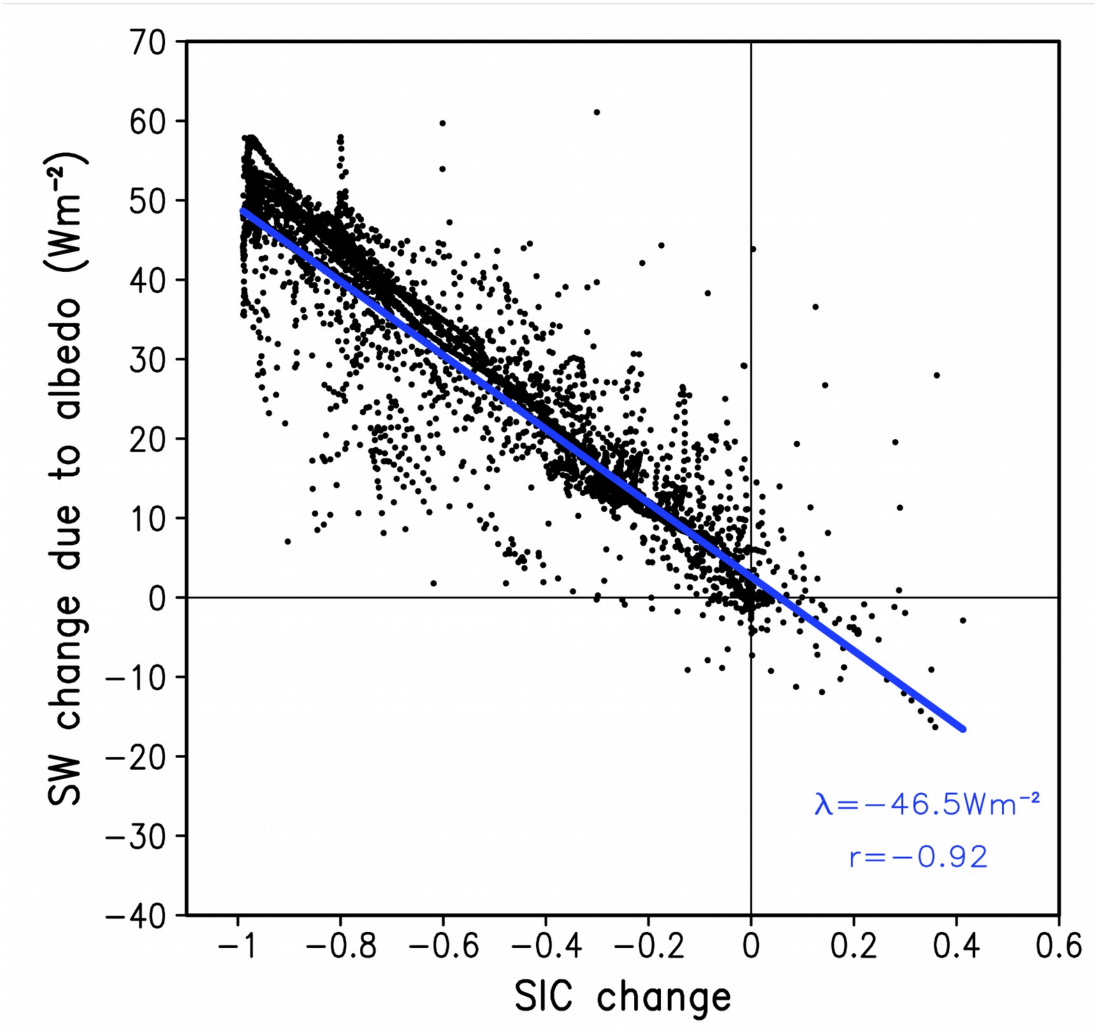

SW change due to albedo (Wm⁻²)
SIC change
λ=−46.5Wm⁻²
r=−0.92

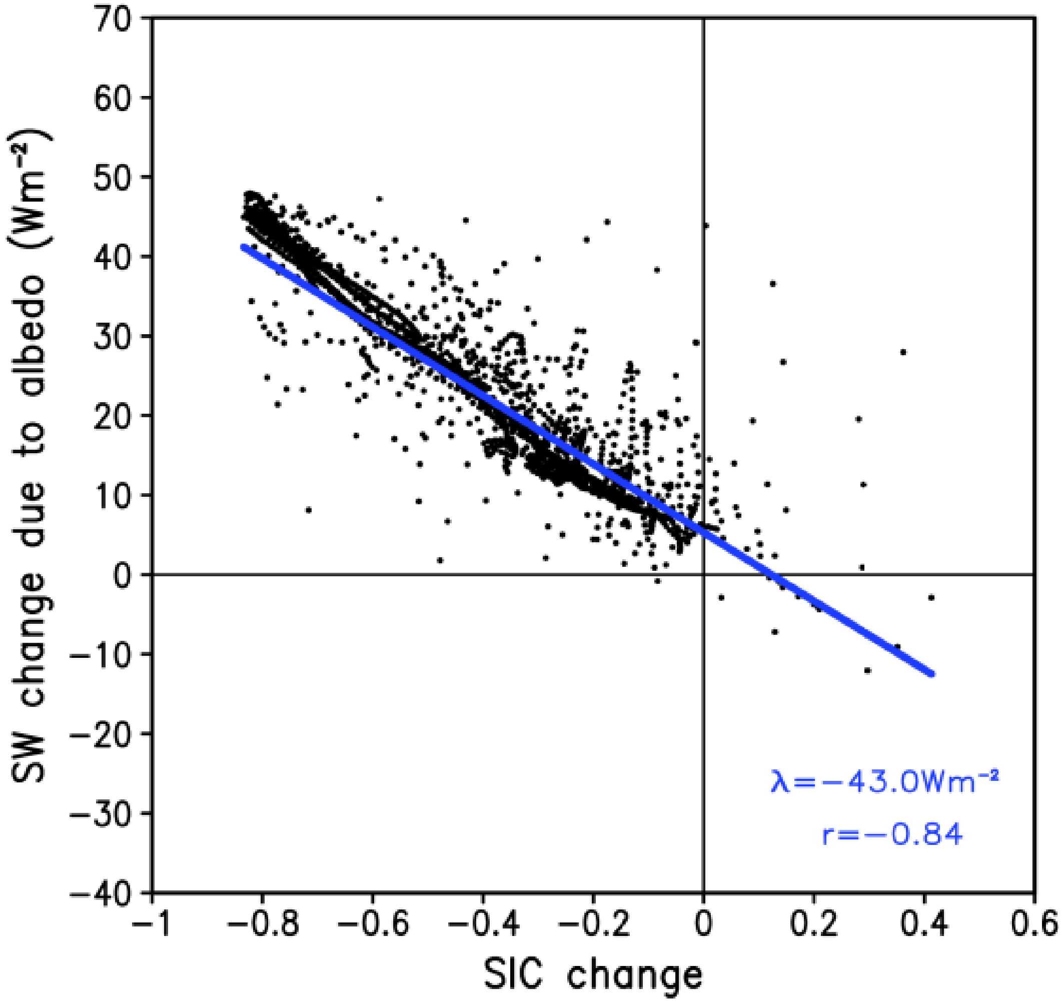

Figure 5. The annual mean net shortwave ~~radiation~~ flux change (Wm^{-2}, positive downward) caused by the albedo effect of sea-ice change averaged over the Arctic Ocean as a function of SIC change. All the change ~~are~~is with respect to the preindustrial period, and each dot represents one grid point value over the Arctic Ocean.

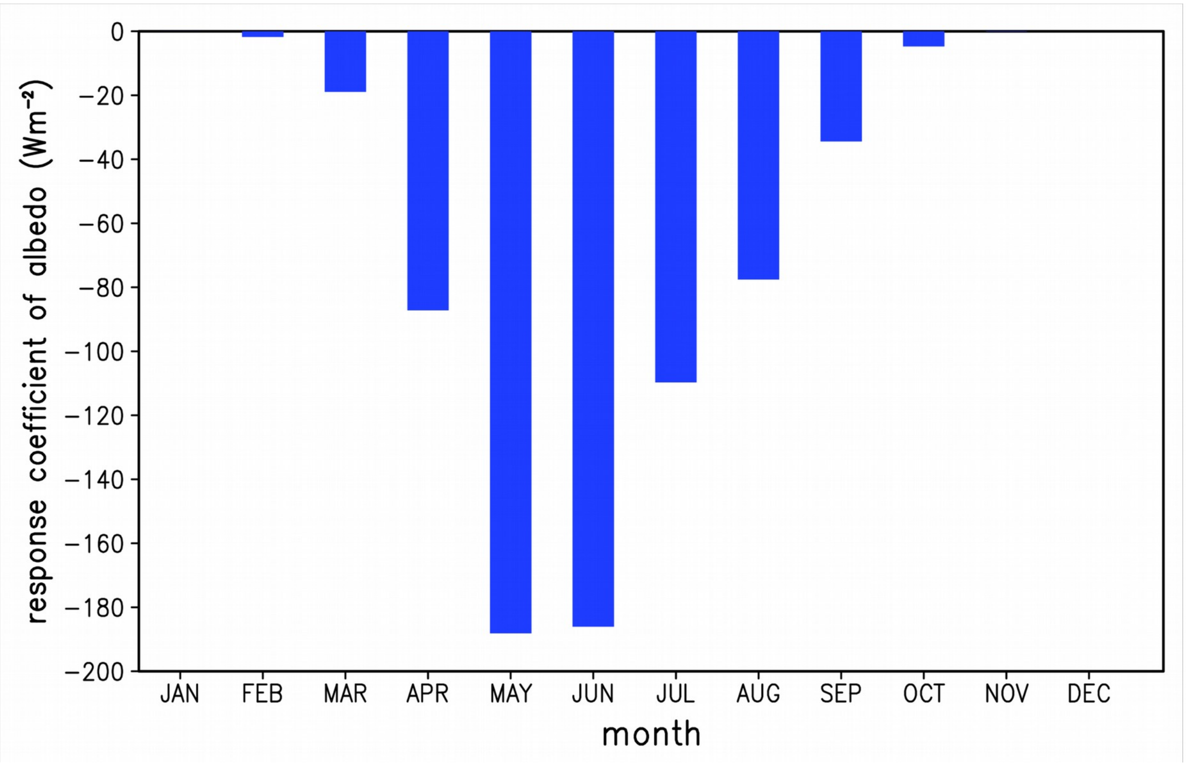

response coefficient of albedo (Wm⁻²)
0
−20
−40
−60
−80
−100
−120
−140
−160
−180
−200
JAN
FEB
MAR
APR
MAY
JUN
JUL
AUG
SEP
OCT
NOV
DEC
month

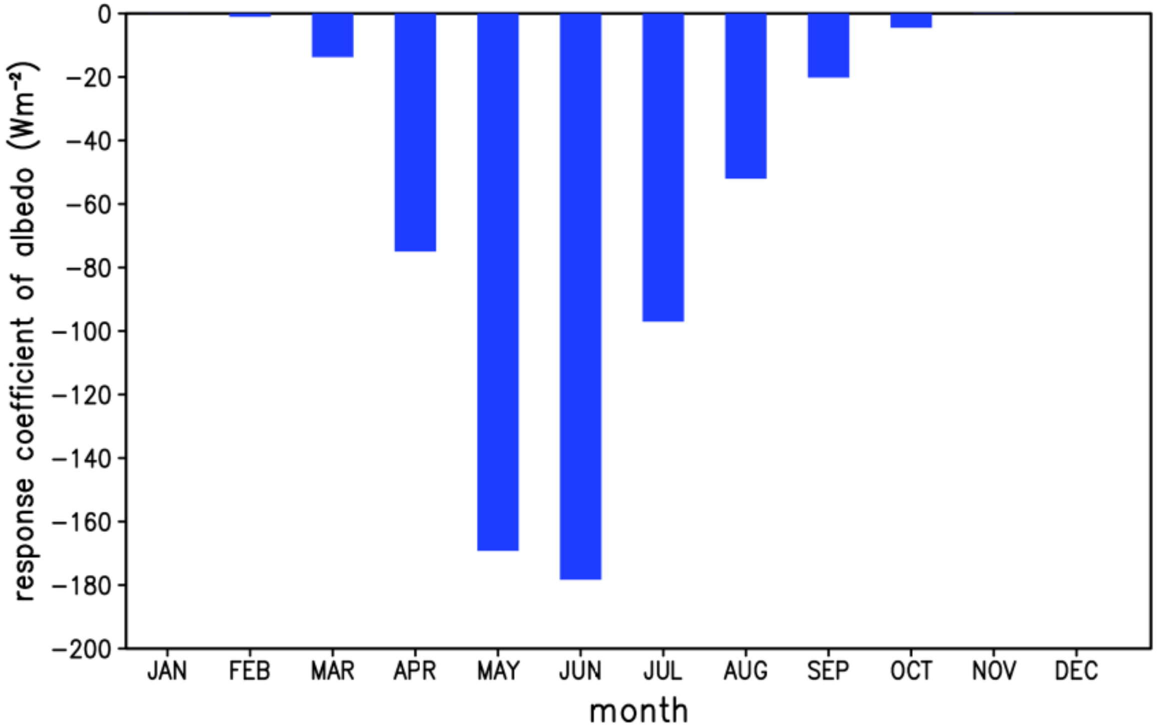

Figure 6. The monthly response coefficients (Wm^{-2}) of net shortwave ~~radiation~~ flux to the albedo effect of sea ~~-~~ice.

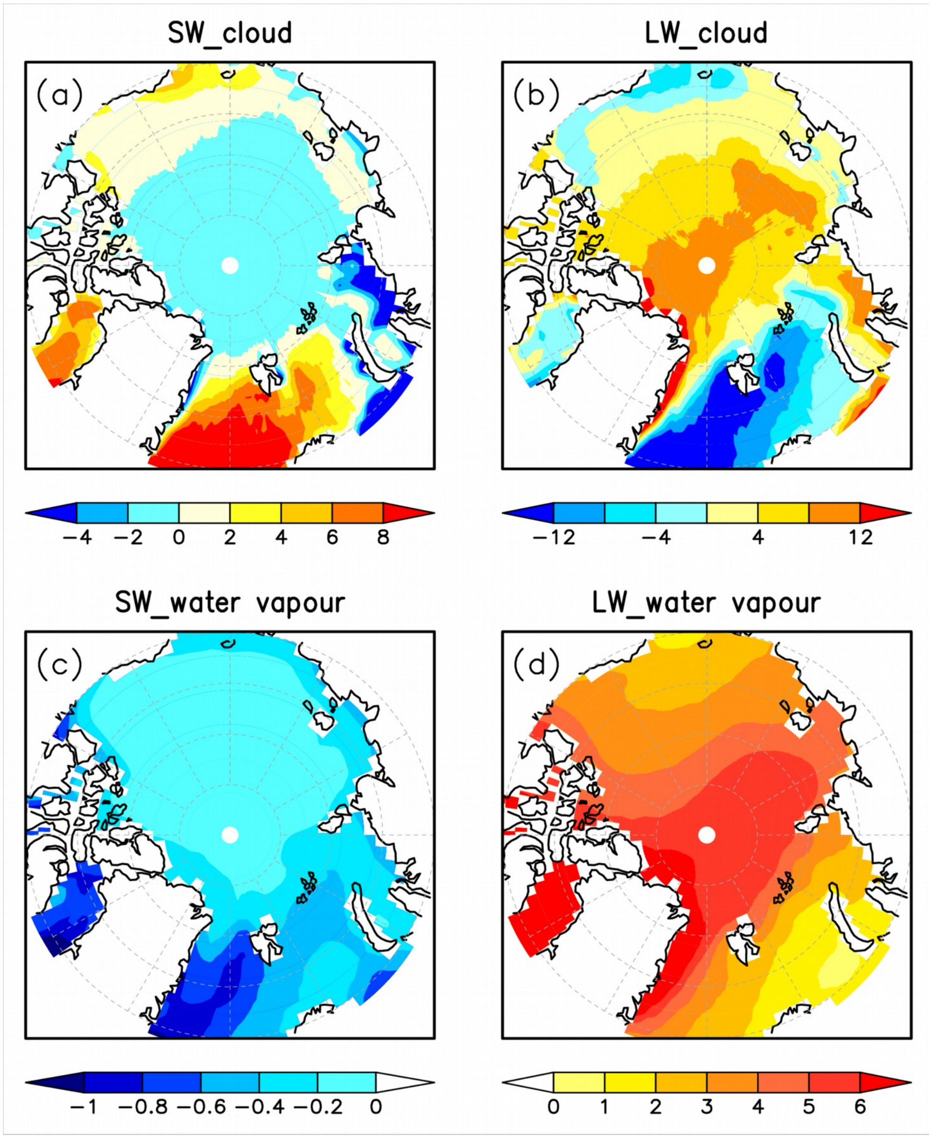

Figure 7. Spatial distributions of the Pliocene annual mean radiation fluxes change (Wm^{-2}, positive downward) with respect to the preindustrial period over the Arctic Ocean. (a) shortwave radiation due to cloud change, (b) longwave radiation due to cloud change, (c) shortwave radiation due to water vapour change, (d) longwave radiation due to water vapour change. Here ~~the~~ , cloud and water vapour change is ~~specified as~~the value before removing the ~~part caused by sea-ice decrease~~remote effects of clouds and water vapour.

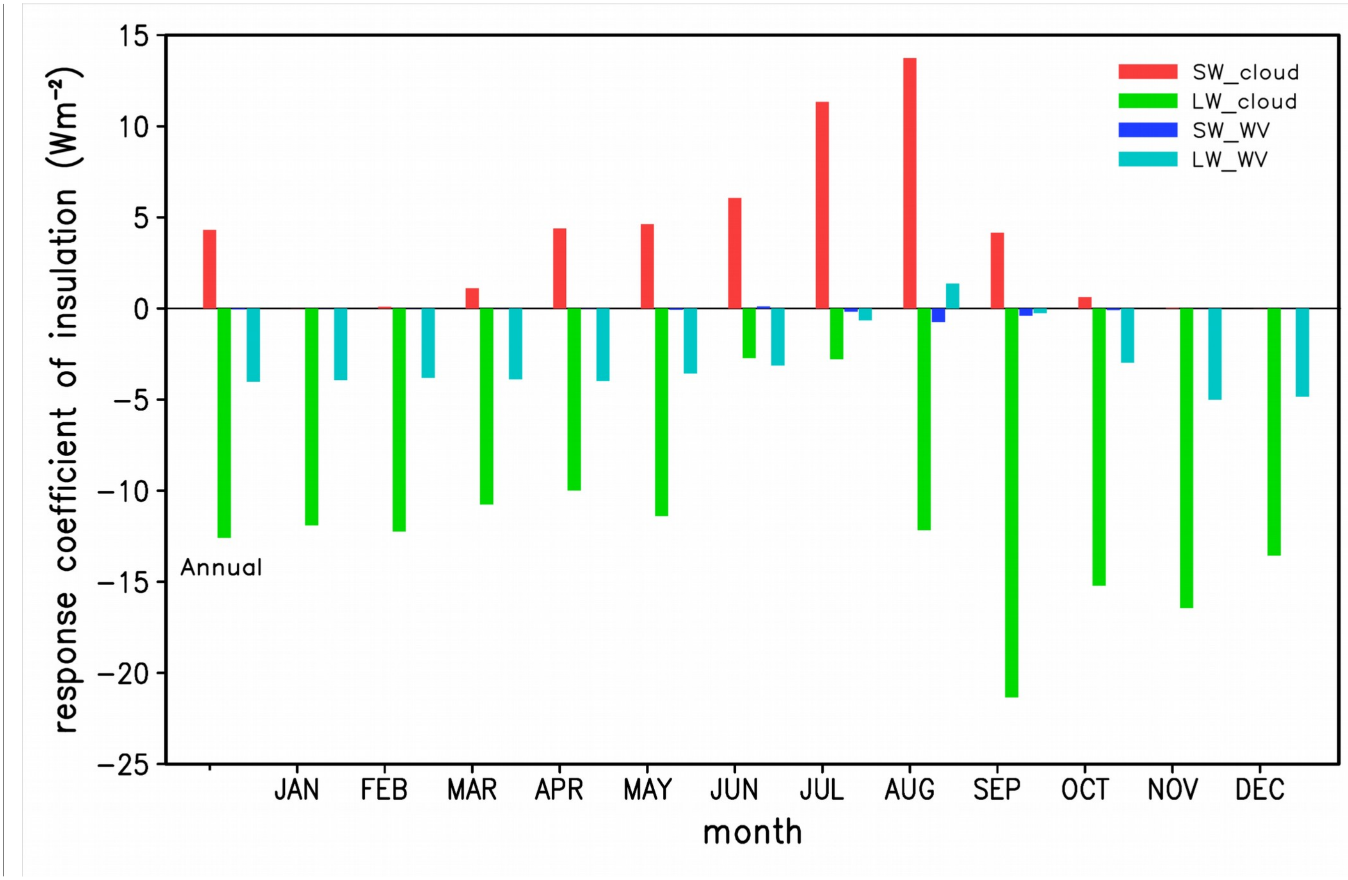

response coefficient of insulation (Wm⁻²)
15
10
5
0
−5
−10
−15
−20
−25
SW_cloud
LW_cloud
SW_WV
LW_WV
Annual
JAN
FEB
MAR
APR
MAY
JUN
JUL
AUG
SEP
OCT
NOV
DEC
month

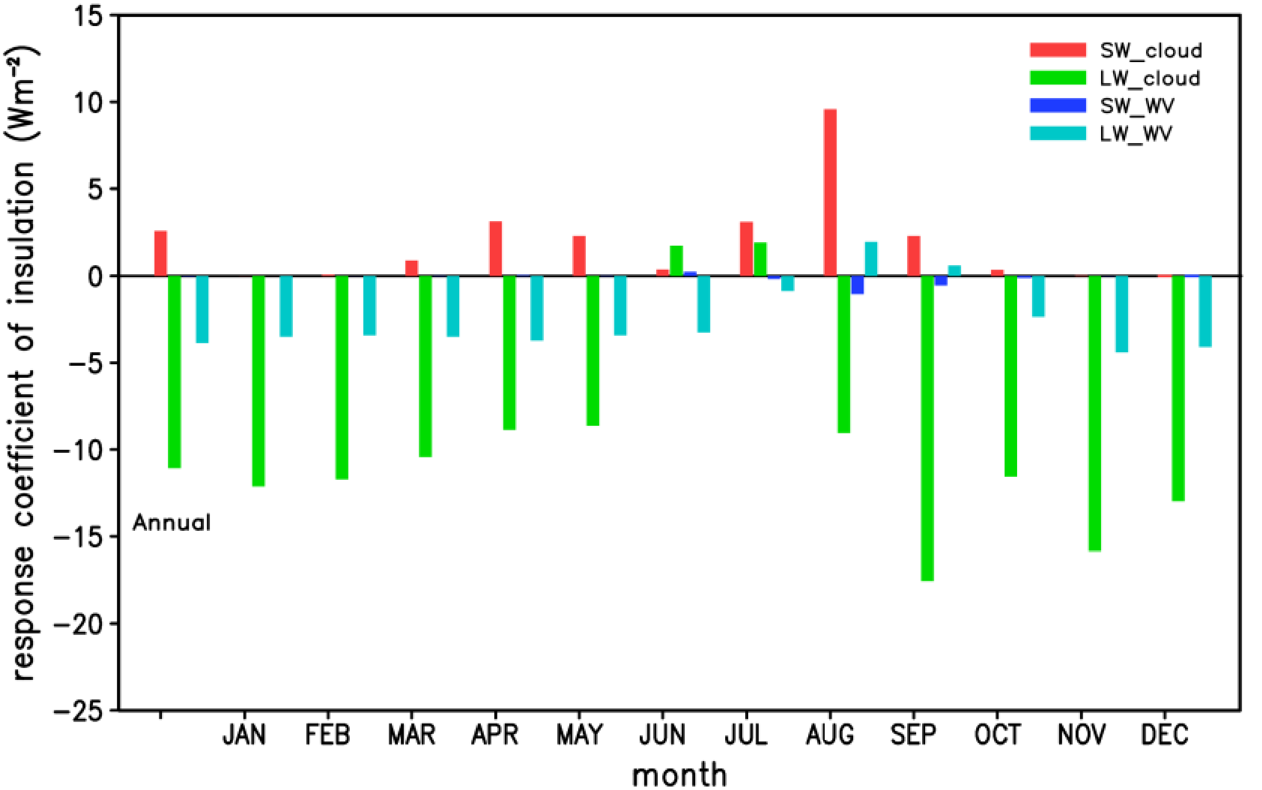

Figure 8. The annual and monthly response coefficients (Wm^{-2}) of net shortwave and longwave radiation flux ~~caused by~~related to cloud and water vapour change to the insulation effect of sea ~~-~~ice. Here, the cloud and water vapour change is specified as the part ~~caused by~~related to sea ~~-~~ice decrease.

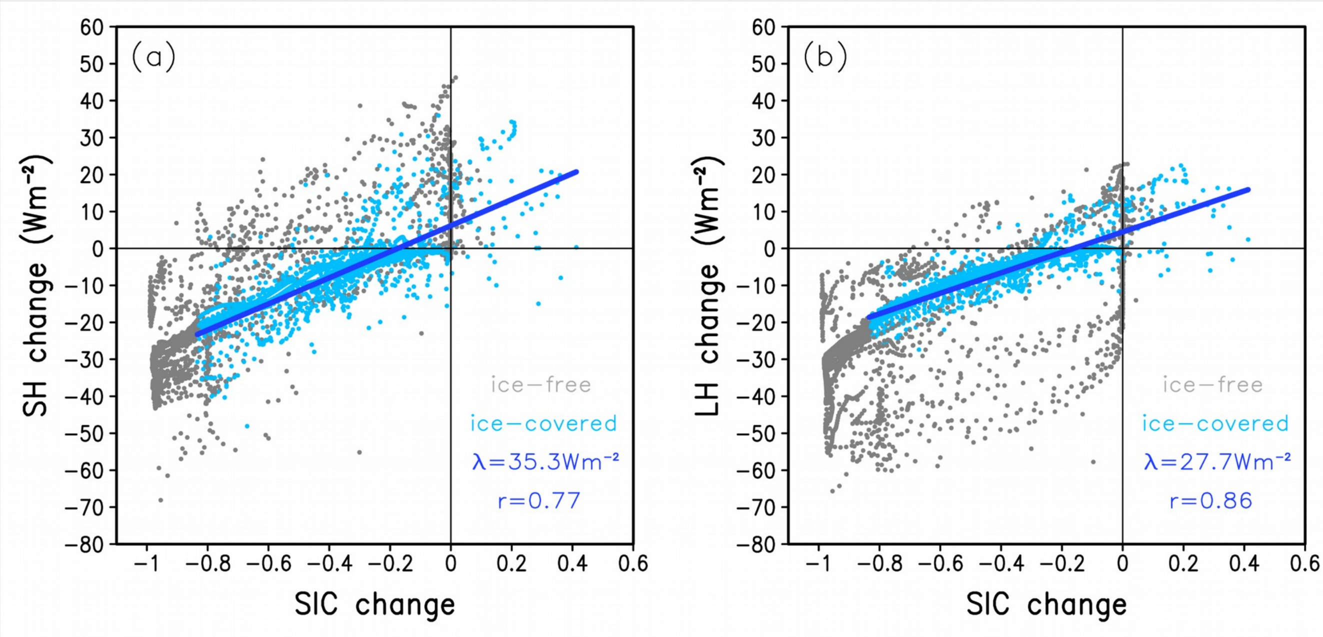

Figure 9. The annual mean sensible and latent heat flux change (Wm^{-2}, positive downward) ~~caused by~~related to insulation effect of sea ~~-~~ice change averaged over the Arctic Ocean as a function of SIC change. ~~All the change~~Pliocene changes shown are ~~with respect~~computed relative to the preindustrial simulation. The ice-free and ice-covered regions here refer to the diagonal hatched and cross-hatched regions in Figure 2c, respectively. The blue line is the linear regression on the ice-covered scatter points, and the response coefficient (λ) and correlation coefficient (r) are just for the ice-covered areas.

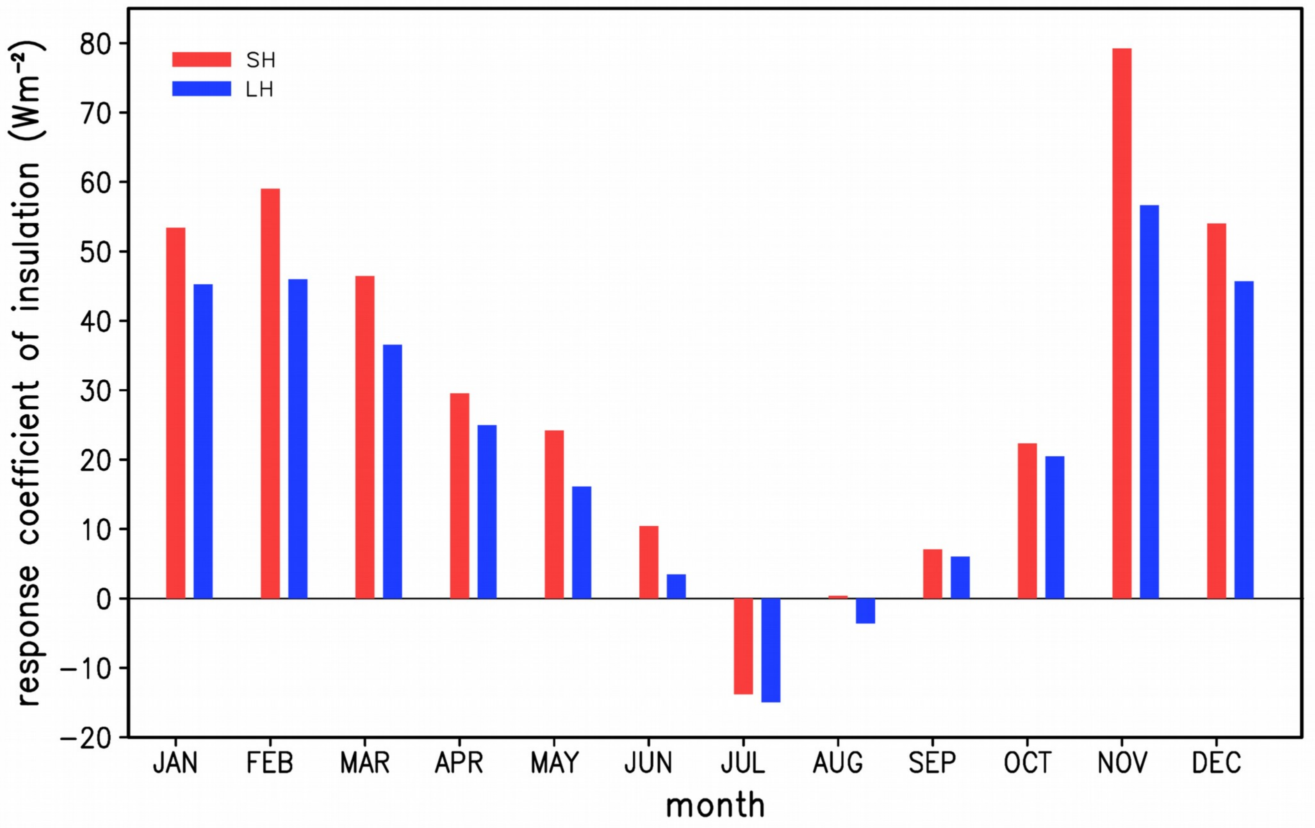

Figure 10. The monthly response coefficients (Wm^{-2}) of sensible and latent heat fluxes to the insulation effect of sea -ice.